International Journal of Biological Macromolecules 209 (2022) 1613–1628

Contents lists available at ScienceDirect

International Journal of Biological Macromolecules

journal homepage: www.elsevier.com/locate/ijbiomac

Review

Ultrasound-assisted fabrication of biopolymer materials: A review

Bowen Cai [a,b], Janine Mazahreh [c,d], Qingyu Ma [e], Fang Wang [a,b,*], Xiao Hu [c,f,g,**]

[a] Center of Analysis and Testing, Nanjing Normal University, Nanjing 210023, China
[b] School of Chemistry and Materials Science, Nanjing Normal University, Nanjing 210023, China
[c] Department of Physics and Astronomy, Rowan University, Glassboro, NJ 08028, USA
[d] Department of Chemistry and Biochemistry, Rowan University, Glassboro, NJ 08028, USA
[e] School of Computer and Electrical Information/School of Artificial Intelligence, Nanjing Normal University, Nanjing 210023, China
[f] Department of Biomedical Engineering, Rowan University, Glassboro, NJ 08028, USA
[g] Department of Molecular and Cellular Biosciences, Rowan University, Glassboro, NJ 08028, USA

ARTICLE INFO

Keywords:
Ultrasound
Cavitation effect
Natural polymer
Biofabrication and modification
Progressive tension on performance

ABSTRACT

There is an urgent need to develop technologies that can physically manipulate the structure of biocompatible and green polymer materials in order to tune their performance in an efficient, repeatable, easy-to-operate, chemical-free, non-contact, and highly controllable manner. Ultrasound technology produces a cavitation effect that promotes the generation of free radicals, the fracture of chemical chain segments and a rapid change of morphology. The cavitation effects are accompanied by thermal, chemical, and biological effects that interact with the material being studied. With its high efficiency, cleanliness, and reusability applications, ultrasound has a vast range of opportunity within the field of natural polymer-based materials. This work expounds the basic principle of ultrasonic cavitation and analyzes the influence that ultrasonic strength, temperature, frequency and induced liquid surface tension on the physical and chemical properties of biopolymer materials. The mechanism and the influence that ultrasonic modification has on materials is discussed, with highlighted details on the agglomeration, degradation, morphology, structure, and the mechanical properties of these novel materials from naturally derived polymers.

1. Introduction

Biopolymers are naturally derived polymers that consist of many units or parts and are usually found in living organisms. Chitin, hyaluronic acid, and starch are polysaccharides that are widely found in nature [1,2] along with cellulose-based plant fibers, such as cotton and sisal [3], and protein-based animal fibers, such as silk, wool and mohair [4–6]. In addition, polylactic acid (PLA), polyglycolic acid (PGA) and their related polymers or copolymers are also naturally derived materials that have been widely studied in recent years [7]. These naturally abundant materials each possess characteristics of richness, renewability, and unique biology that is favored by many studies [5] (Fig. 1). For the regeneration and modification of these natural polymer materials, more complicated fabrication approaches such as the acid-salt method [6], the water-based method [8] and the chemical grafting [9] are often implemented.

In addition to the well-known medical applications, ultrasound has been increasingly used for the fabrication and modification of new materials in recent years due to its high efficiency, easy operation, repeatability and controllability, including its involvement with naturally derived polymer materials [10]. Ultrasound involves a series of sparsely populated dense longitudinal waves that are generated through the propagation of a medium to construct a divergent, flat, or focused sound field to generate mechanical vibration energy. When acting on a material, it will give rise to mechanical, acoustic, thermal, chemical, and biological effects [11], which together modifies the physical properties of the material. Studies have shown that ultrasonic energy can be applied to the field of textile dyes to accelerate the interaction between the dye and the fiber, reinforcing fabric dyed color [12]. This application was shown to improve adhesion, wash fastness and lightfastness [12]. Furthermore, the use of ultrasound could function to alter the mechanical properties of nanofibers, microfibers, and gelling materials as a drug delivery vehicle for target therapy [13].

This review serves as a summary of research progress in recent years

* Correspondence to: F. Wang, Center of Analysis and Testing, Nanjing Normal University, Nanjing 210023, China.
** Correspondence to: X. Hu, Department of Physics and Astronomy, Rowan University, Glassboro, NJ 08028, USA.
E-mail addresses: wangfang@njnu.edu.cn (F. Wang), hu@rowan.edu (X. Hu).

https://doi.org/10.1016/j.ijbiomac.2022.04.055
Received 10 January 2022; Received in revised form 15 March 2022; Accepted 6 April 2022
Available online 20 April 2022

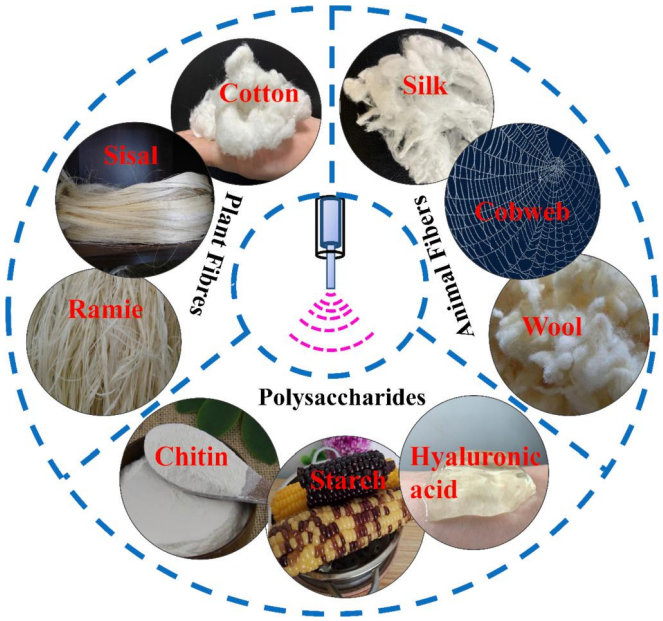

Fig. 1. A scheme showing ultrasound applications using various biopolymer materials. Pictured raw biopolymer materials include plant fibers (cotton, sisal, ramie), animal fibers (silk, cobweb, wool), and polysaccharide substances (chitin, starch, hyaluronic acid), with applications towards biological tissue scaffolds, artificial stents, wood modification, drug package and delivery, environmental protection products, beauty products, antibacterial fabrics, artificial ligament and gel materials.

on ultrasonic fabrication and modification of biopolymer materials. The general principle of ultrasonic theory is discussed along with its field applications. This review will provide a comprehensive study for the use of ultrasound to create new biomedical and sustainable materials using various naturally derived biopolymers.

2. The theory behind ultrasound

The phenomenon known as cavitation was first discovered in 1895 when Thornycroft and Barnaby observed a collapsing of bubbles that were caused by hydrodynamic cavitation, producing a strong pressure and temperature gradient in the local vicinity [13]. In 1917, Lord Rayleigh provided a simple derivation formula to calculate the pressure inside the fluid during the collapsing process, describe the cavitation phenomenon in the incompressible fluid, and thus established the first mathematical model [14], using the following Formulas (1) and (2):

$$\frac{u}{U}=\frac{R^2}{r^2} \tag{1}$$

$$\frac{1}{2}\rho\int_{R}^{\infty}u^2\cdot 4\pi r^2 dr = 2\pi\rho U^2 R^3 \tag{2}$$

where R is the bubble radius, U is the surface vibration velocity at time t, u is the velocity at any distance r ($>R$) of the bubble from the center, and ρ is the density of the medium. Formula (2) describes the kinetic energy of the bubble. The sound wave is transferred to the bubble energy through the liquid medium, causing it to expand during the negative sound pressure period and contract during the positive sound pressure period. The sound propagation process will cause the energy in the bubble to accumulate, and the bubble oscillation radius continues to grow. When the bubble resonance is reached, the sound pressure exceeds the threshold, the bubble collapse occurs and releases an intense quantity of energy forming ultrasonic cavitation [15]. In 1927, Loomis and Richards et al. [16] first reported the ultrasonic cavitation in ether on the basis of the above model theory. In 1937, Brohult et al. [17] reported the use of ultrasonic cavitation to degrade biopolymers such as hemocyanin molecules. In 1961, Naude and Ellis discovered that microjets would cause pitting on the surface of materials. Through these historical developments, the notion that ultrasound could be applied to the field of materials science was increasingly accepted across the scientific community. Additionally, it was found that when the symmetrical bubble propagates from the collapse point to the outer diameter of surrounding fluid, the energy generated could be used to accelerate the mass transfer rate between the interfaces. Simultaneously, the reaction temperature and pressure will rise, the temperature vaporizing any participating liquid reactants, and the high pressure increasing the efficiency of the multiphase reaction [18]. During the ultrasound process, the rupturing cavitation bubbles are affected by the amount of water vapor that enters the bubbles during bubble formation. The more water vapor that enters the bubbles, the stronger the buffering effect of the collapse. Therefore, as the system temperature rises, the ultrasonic power will increase. The further solution of acoustic power P on the basis of adiabatic conditions can be derived from Formula (3) [19]:

$$P=\left(\frac{\mathrm{d}T}{\mathrm{d}t}\right)_{t=0}c_p m \tag{3}$$

where C_p is the heat capacity of the solution, m is the total mass of the solution, T is the temperature, and t represents the time. If the power is emitted from the probe tip and propagated into the system, in order to further obtain the sound power per unit area [20], the power intensity generated by the ultrasonic source is given by Formula (4):

$$I=P_{\mathrm{a}}^2(2\rho\cdot C)^{-1} \tag{4}$$

where I represents the sound intensity, ρ and c are the medium density and sound velocity, and P_{a} is the amplitude of sound pressure, which is related to the time t and the frequency f, as shown in Formula (5):

$$P_{\mathrm{a}}=P_{\mathrm{a},max}sin(2\pi ft) \tag{5}$$

where $P_{\mathrm{a,\ max}}$ is the maximum sound pressure value [21], which is proportional to the propagation time and the frequency of ultrasonic waves.

Sound pressure P_{a} can be further used to determine the maximum bubble size of cavitation bubbles [22], and the size of bubbles generated by resonance can be related to the frequency [15], as shown in Formulas (6) and (7):

$$R_{\mathrm{r}}=\sqrt{\frac{3\gamma P_{\infty}}{\rho\omega^2}} \tag{6}$$

$$R_{\max}=\frac{4}{3\omega_a}(P_{\mathrm{a}}-P_{\mathrm{h}})\left(\frac{2}{\rho P_a}\right)^{1/2}\left[1+\frac{2}{3P_h}(P_{\mathrm{a}}-P_{\mathrm{h}})\right]^{1/3} \tag{7}$$

where R_{r} represents the bubble size, $R_{\max}$ is the maximum size of the bubble, γ is the specific heat ratio of the gas inside the bubble, P_{∞} is the ambient liquid pressure, P_{h} is the external (hydrostatic) pressure, ρ is the liquid density, and ω is the angular frequency of the ultrasound. According to the above formulas and experimental results, there will be an optimal power density in the ultrasonic process to obtain the maximum reaction rate.

It can be seen that the intensity of ultrasound [23,24], temperature [25] and frequency [26,27], as well as the surface tension of different liquids [28], will affect the effect of ultrasonic cavitation in biopolymer materials, which are described in detail below.

3. Factors that influence cavitation

3.1. Intensity

In general, when under the same area, the strength of ultrasonic power is directly proportional to the amplitude of the soundwave, which causes the intensity of the cavitation bubble collapse to increase. Therefore, when the ultrasonic intensity of a liquid increases, the cavitation intensity increases, thus leading to a greater sonochemical effect in the presence of more bursting bubbles with a faster pulsation and collapse. When the ultrasonic intensity reaches its limit, the cavitation has the tendency to saturate, and an excessive increase in intensity will produce bubbles that increase the scattering attenuation and reduce the cavitation intensity [19]. If the intensity increases past a critical point, OH radicals will form in the solution reaction, which will promote a rapid degradation of the substances involved. The ultrasonic propagation is mainly nonlinear to a certain extent [29].

In general, the actual ultrasonic intensity (W/cm^2) can be represented by the Formula (8) [33]:

$$I = P/(\pi r^2) \tag{8}$$

where P is the actual power dissipation, r is the radius of the ultrasonic probe tip (cm), and I is the ultrasound intensity.

Several studies [13,23,24,30–34] have defined the relationship between an increase of ultrasonic power (W) or ultrasonic intensity (W/cm^2) and its effect on the fabrication of materials. Dükkanci et al. [30] studied the effects of ultrasonic power and H_2O_2 on the degradation of oxalic acid. It was found that the burst of cavitation bubbles would become violent at higher acoustic amplitudes. Under the same ultrasonic area, the power was increased from 70 W to 95 W, forming bubbles that gradually developed into a large acoustic chemical reaction. The authors found that this action promoted the degradation of oxalic acid from 2% to 14%. When the ultrasonic power increased from 95 W to 120 W, under the same ultrasonic area, the degradation of oxalic acid was not increased. Zhang et al. [31] revealed that when the ultrasonic power increased from 60 W to 423 W, under the same ultrasonic area, the molecular weight of citrus pectin decreased from 401 kDa to 261 kDa, while when the ultrasonic intensity continually increased to 544 W, the molecular weight was stable at around 267 kDa. Hao et al. [32] discovered that when the ultrasound intensity was greater, there was a more profound inhibitory effect on the overall growth of cyanobacteria, although the difference was minimal. The conclusive results showed that 40 W power was the most economical and effective power for ultrasound. When the power was increased to a certain level, the cavitation bubbles became too large to collapse under higher power, or collapsed weakly, which resulted in a decrease in the cavitation effect. Qiu et al. [33] discovered that a higher ultrasonic intensity, such as 104.7 W/cm^2, can lead to methoxylation of the side chains in citrus pectin molecules, causing the intermolecular and intramolecular hydrogen bonds to break. Without the presence of hydrogen bonding in the molecular structure of the pectin solution, the coiled chain structure will transition from a semi-flexible to flexible. Wang et al. [34] studied ultrasound for the use of dye. It was found that when the ultrasonic power increases from 0 to 200 W, dye uptake increased from 5% to 25.5%. Additionally, higher ultrasonic power can also improve the permeability of wood, promoting the activation of dye molecules, making more dye molecules penetrate wood, and increasing the dye uptake rate. Wood is a complex polymer material that contains high molecular compounds. Rudak et al. [35] furtherly pointed out that the alternating stresses from intensive ultrasound action on wood leads to vibrational deformations of these compounds, causing a rupture of the bonds between fibers and irregularities in the orientation of the macromolecular chains. When wood was compacted in the ultrasonic field with an intensity of 3–10 W/cm^2, its maximum density was found to reach up to 1.45 g/cm^3 [35], which is equal to the mechanical high rupturing capacity of 60–63 N/mm^2. There are several potential applications of such wood, such as for the manufacturing of friction parts, thrust bearings as a primary example [35]. These results suggest that the mechanical properties of polymer materials change directly with an increase in ultrasound performance. However, wood consists primarily of cellulose, hemicellulose, and lignin. Therefore, ultrasound at a high intensity can cause an overall reduction of the total cellulose content in wood, leading to a partial degradation of wood macromolecules [36]. For example, Qian et al. [37] found that in a material ultrasonically treated with a power of 240 W and a frequency of 28 kHz, its holocellulose content decreased by 9.55% when in compared with a control group. Both stable and transient cavitation bubbles can result through ultrasonic intensity. Differences in ultrasonic intensity can provide nano-bioengineered materials that possess a high stability, small particle sizes, and narrow polydispersity. Such conditions allow for improved solubility and antioxidant and mechanical properties in biomaterials [38]. All the above-mentioned findings suggested that the choice of ultrasonic intensity is unique for different material fabrication and modification processes and should be carried out according to the specific material used in the ultrasound study.

3.2. Frequency

In a liquid solution, cavitation is highly dependent on frequency. Additionally, the strength of bubble bursting (i.e., released energy) and the maximum bubble size before bursting (resonance size) are related to each other according to Formulas (4)–(7). Generally, the ultrasonic cavitation spectrum is divided into low frequency (16–100 kHz), intermediate frequency (100–1000 kHz) and high frequency (above 1000 kHz). Studies have shown that low frequency ultrasound will produce larger resonance bubbles [15]. When the bubbles collapse, strong physical effects will occur such as local shear and high temperature, as well as the generation of high energy on the order of 10–1000 W/cm^2, which can be used in the homogeneous synthesis of materials [39], polymerization [40] and cell disruption [41]. Kadem et al. [42] found that the lower the ultrasonic frequency, the more uniform the energy distribution, and the lower frequency (40 kHz) is more conducive to the composite regeneration of polyvinyl alcohol (PVA) and titanium dioxide (TiO_2) materials. The results of the study suggested that the mechanical properties of polyvinyl alcohol (PVA) could be improved using an ultrasonic frequency of 53 kHz. The study also resulted in an increased tensile strength and elongation of 15.3 kgf/cm^2 and 99.63% respectively [43]. Intermediate frequency ultrasound will produce the most "sonochemically active" bubble groups, leading to efficient free radical production, which is the most common area for chemical modification. For example, the use of this ultrasonic frequency to promote the decomposition of micelles and polymer aggregates in the dye bath into a uniform dispersion can enhance the contact between the dye and the fibril, thus accelerating the diffusion rate of the dye in the fiber effect [44]. The bubbles produced by high-frequency ultrasound are very small, and the proportion of bubbles cavitation decreases due to the increase of the cavitation threshold, suggesting that the physical effects when they collapse will be relatively mild [45]. This mode is suitable for selective particle separation while maintaining the integrity of the separated product [46]. Albermany et al. [47] studied the mechanical properties of polyvinyl alcohol-palm fiber composites with frequencies ranging from 25 to 50 kHz. It was found that as the frequency increases from 25 kHz to 50 kHz, the bulk modulus of the composite material drops from 5×10^5 dyne/cm^2 to 3×10^5 dyne/cm^2 after ultrasonic action. The authors theorized that in the region of 20 kHz–100 MHz, ultrasonic waves are mechanical vibrations that propagate through small displacements of atoms and chain segments around their equilibrium positions [48]. Therefore, the ultrasonic forces acting on polymer chain segments and between their molecular chains possess the ability to create displacements to the neighboring zones [48]. The propagation of ultrasound produces randomly coiled polymer chains closer to each other in

polymer, making the molecules more compressible. In a confined manner, the polymer molecules will have restricted movement, leading to fiber composites. The elasticity of the material decreases as the bulk modulus decreases. Additionally, it was found that when the ultrasonic frequency is increased to 20 kHz, the size of the emulsion droplets increased from 0.83 μm to 1.02 μm [49]. Wu et al. [50] confirmed that at an ultrasonic frequency of 20 MHz the water molecules penetrated into the amorphous region, causing the polymer to swell. This resulted in an increase in the thickness of the material. When the polymer degraded, the shorter molecular chain was ruptured, and the remaining space was filled with water molecules, resulting in a decrease in the bulk modulus. Therefore, low-frequency ultrasound was found to cause polymerization and depolymerization, and the change from depolymerization to polymerization is determined by the nature of cavitation. At lower ultrasonic frequencies (for example, 20 kHz), the mechanical action produced by ultrasound can be used, and when the ultrasonic power is increased (>500 kHz), the main action is caused by free radical reactions [17,41,42,44].

3.3. Temperature

High liquid temperature is conducive to cavitation. This relationship is explained by the inverse relationship between temperature and viscosity. When the temperature of a solution is elevated, thereby increasing vapor pressure, the viscosity coefficient and surface tension of the solution decreases, thus leading to a formation of cavitation bubbles. In the ultrasonic cavitation process, cavitation microbubbles composed of dissolved gas and water vapor continuously form, grow, and implode, producing physiochemical effects within a solution [12,45]. The collapse of cavitation bubbles occurs rapidly with limited heat loss. A gradual rise in temperature increases the liquid-vapor pressure of the solution, resulting in the dissociation of water vapor molecules, promoting the formation of free radicals, and improving the overall effect of ultrasonic cavitation. Through ultrasonic wave, rapid expansion, sudden closure, and oscillation will occur in the tiny bubble nuclei in the liquid [12,45].. At elevated temperatures ranging from 60 to 70 °C, the vapor pressure in the bubble will increase acutely, which will close the bubble again, enhancing the buffering effect and thereby weakening the cavitation effect [12,51]. A study by Yen et al. [52] exemplified this effect when the intrinsic viscosity of a polyacrylamide solution decreased from 3 dl/g to 1 dl/g when the ultrasonic temperature was increased from 20 to 50 °C at 550 W power. Wang et al. [53] studied the effect of the synergistic effect of glucoamylase and ultrasound on starch hydrolysis. The findings suggested that the high temperature brought by ultrasound reduced the enzymatic hydrolysis efficiency and the thermal stability of glucoamylase, accelerating the heat inactivation of glucoamylase. Additionally, high temperature hinders the ultrasonic cavitation effect due to the collapse of cavitation bubbles with higher strength and lower temperature. Hernandez et al. [54] analyzed the relation of the cavitation power output and temperature. The cavitation effect between 20 °C and 70 °C is minimal, but when the temperature exceeds 70 °C, the cavitation capacity will drop sharply. Some studies [49] found that a slightly increased temperature will overcome the cohesive force of the ultrasonic keratinocyte growth medium (KGM) tear fluid, which generated cavitation bubbles. In contrast, ultrasonic cavitation increased the temperature and promoted the intensification of molecular activities in the solution. The higher temperature caused by ultrasound increased the number of cavitation bubbles and the surface contact area, reducing the viscosity and density of the liquid, and accelerating the mass transfer rate. For example, H^+ catalysis in the system accelerates the degradation of konjac glucomannan. Ticha et al. [55] used natural colorants extracted from red cabbage to improve the dyeability of cotton fabrics and found that when the dyeing temperature is increased from 30 °C to 95 °C, the most effective results were under the action of 500 W ultrasound. Yang et al. [56] showed that ultrasound can be used to assist the extraction of polysaccharides from *Hovenia dulcis*, and the maximum extraction rate was obtained when the temperature reached 65 °C.

Therefore, ultrasonic cavitation will cause the temperature of the system to rise, which is more conducive to the generation of cavitation. However, at the critical temperature of a specific material, cavitation will be weakened.

3.4. Liquid surface tension

The characteristics of a material are significant for cavitation. For example, the viscosity of the liquid affects its surface tension. The larger the surface tension of the liquid, the more difficult it is to produce cavitation [52–54]. Since the coefficient of the liquid is difficult to produce cavitation bubbles and the propagation loss is large, cavitation production is difficult. However, the amount of dissolved gas in the liquid influences the bubble nucleation rate. The higher the solubility of the gas, the lower its surface tension. Under ultrasonic action, reducing the surface tension resulted in a significant increase in bubble stability [54], and the nucleation rate was increased [57]. Researchers have suggested that ultrasonic cavitation is primarily caused by highly eroded bubble clusters [58]. The reduction of surface tension promotes the instability of bubble growth and collapse, breaking the bubbles into smaller bubbles with less erosive power. The same study reported that the surface tension of the liquid has a strong effect on the size and number of bubble clusters, with the average bubble diameter coinciding with the relative erosion rate. This effect is of upmost importance in the early stages of bubble formation and at later stages of bubble collapse. Sheng et al. [59] used 20 kHz and 90–480 W ultrasonic power to study the foaming ability of egg whites and found that the increase in power reduced the surface tension of the egg white from 59 to 54 mN/m, exhibiting the highest foaming capacity. Reducing the surface tension was found to be conducive to the rapid diffusion of protein molecules to the gas-liquid interface, and it was found to be more conducive to the adsorption and in the stretching and rearrangement of protein molecules on the interface. Camerotto et al. [60] studied the effect of a nonionic surfactant on air bubbles under different oxygen saturations of 90–105%. It was found that by adding a surfactant, a body surface tension of 45 mN/m was obtained along with a better cavitation effect, and in the presence of non-ionic surfactants, the number of active cavitation bubbles increased. The cavitation effect was found to be greater in comparison with water solvents. Thus, the surface tension of the liquid does have a considerable effect on the ultrasonic cavitation.

4. Ultrasound for the modification of biopolymer materials

Ultrasound has become an increasingly studied topic in recent years due to its wide range of uses. Ultrasound does not cause chemical pollution, making it extremely valuable in the field of new materials, particularly for naturally derived polymer modification. Studies have shown that ultrasound is compatible to pair with existing material preparation methods, as it plays an important role in the material agglomeration, morphology, crystallinity, degradation, and mechanical properties [51] (Fig. 2). The use of ultrasonic technology can successfully separate nanofibers from wood, bamboo, wheat straw and flax fibers [50–52]. Zhang et al. [61] found that ultrasound can also accelerate the extraction of micro-nano keratin from wool fibers (Fig. 2a). Vallejo-Domínguez et al. [62] observed that under the action of ultrasound, the polymer particles appeared dense and multi-layered. As time increases, the surface of the polymer corrodes. After 35 min of sonication, more dense particles will be observed (Fig. 2b). Another study [63] also pointed out that after alkali-treated sisal fiber is treated with 1000 W high-intensity ultrasound for 90 min, the aspect ratio of the fiber will be greatly improved, thereby improving the mechanical and thermal properties of fiber-reinforced polymer composites (Fig. 2c). Chen et al. [64] combined 160 W power ultrasound with different conditions such as copper ion and hydrogen peroxide and discovered that the synergistic

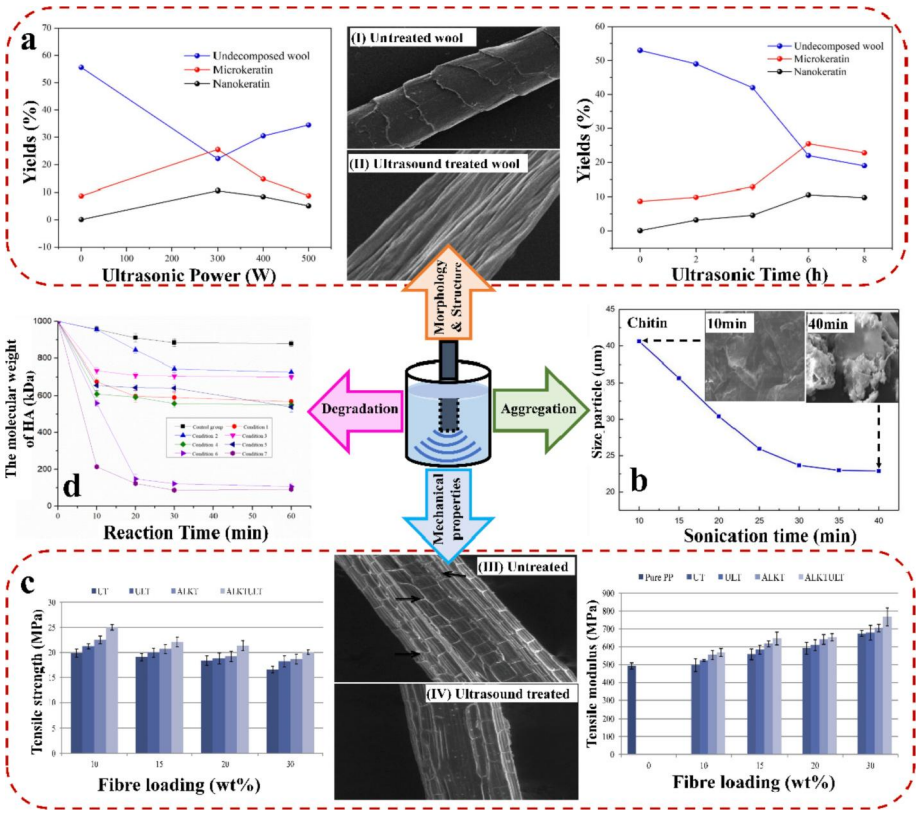

Fig. 2. The effect of ultrasound on material agglomeration, degradation, structure and morphology, and mechanical properties. (a) Ultrasonic action transformed wool and microkeratin from macroscopic to microscopic scale, and the images of (I) untreated and (II) treated wool. (b) Chitin nanofibers were prepared under the ultrasound. (c) Ultrasound treated (ULT), Untreated (UT), Alkali treated (ALKT) and combined alkali and ultrasound (ALKT-ULT) treated sisal fibers, and the morphology of (III) untreated and (IV) treated fiber. (d) Comparison of the degradation efficiency of hyaluronic acid under different ultrasonic conditions. (a), (b), (c), (d) are reprinted with permission from Ref [53,61,63,64]; copyrights (2020) Elsevier, (2021) Elsevier, (2017) Elsevier and (2019) MDPI respectively.

effect produced by the combination of ultrasound and other conditions would promote the degradation of hyaluronic acid. After 30 min of ultrasound, low molecular weight hyaluronic acid with a molecular weight of 74.9 kDa can be obtained (Fig. 2d). In recent studies, the modified materials showed better thermal performance and higher crystallinities. Additionally, studies showed that ultrasound can promote emulsification and polymerization, crosslinking protein chains to form protein microspheres that can be used to control drug release in biological systems [53,54].

Ultrasonic manipulation has been proved to be efficient in the improvement of the compatibility of two-phase materials, making it an important method for the preparation of chemical reactions. Therefore, ultrasound technology has great advantages in promoting the application of naturally derived polymer materials in the fields of biomedicine and material engineering. Table 1 lists the main parameters, ultrasound modified biopolymer materials, and their related application fields.

4.1. Modification of material morphology and structure

Ultrasonic cavitation can be used to prepare materials of different forms, such as hydrogels and nanofibers. Hydrogels are polymer materials that possess a three-dimensional network structure. These materials have become a rising topic across the scientific community due to the strong adsorption performance, green chemistry, and specific functions that hydrogels display. In recent years, it has been discovered that some biconical dihydrazide-derived organogel molecules that cannot be formed into gels by traditional heat treatment methods can form gels under ultrasound stimulation, these are called ultrasound-induced gels [65]. Additionally, it was found that ultrasound-assisted polymerization along with the graft modification method can obtain gels with a better adsorption capacity [66]. For example, ultrasound was utilized to induce an aqueous protein solution into forming a gel rich in β-sheet structure [65]. Ultrasound was also used to enhance the ability of protein chains to quickly and uniformly bind to wool keratin molecules [67]. Using chitosan and betulin as raw materials, an eco-friendly chiral hydrogel was prepared using ultrasound, which was applied to the separation of enantiomers [68]. The ultrasound process initiates an imidization reaction based on the betulinic acid, forming a supramolecular chiral skeleton. The betulinic acid skeleton and chitosan bond to synthesize ordered clusters, thereby inducing the formation of hydrogels. The speed of formation in the hydrogels, or gelation speed, is highly controllable. This is done by adjusting the ultrasonic parameters such as time and amplitude. In a recent study, the ultrasonic time was increased from 10 s to 30 s, and the gelation speed had a notable decrease from 121 min to 3.8 min. In the same study, when the ultrasonic amplitude was increased from 6% to 14%, the gel time was reduced from 60 min to 20 s [59]. It is interesting to note that ultrasound can initiate polymerization in aqueous monomer solutions without the presence of an initiator. This was discovered by Rokita et al. [69], in a study that utilized ultrasound to create a water-soluble three-dimensional network of covalently linked biopolymer chains. After 30 s of ultrasound at 622 kHz, the gel formed. As shown in Fig. 3a, ultrasonic cavitation, OH radicals began to populate. Fig. 3b displays the initiation of the polymeric reaction, and Fig. 3c presents the formation of the self-assembled, natural hydrogel structures. Wang et al. [70] also successfully used chitosan and polyvinylpyrrolidone in a study to prepare an interpenetrating polymer network hydrogel under 500 W ultrasonic conditions in order to promote radical polymerization. These studies together suggest that a rapid gelation is induced by ultrasound, proving this method to be valuable in the field of medical materials [58].

Biopolymer based nanofibers can be extracted from natural fibers that are strong and highly flexible. These nanofibers possess unique characteristic that make them highly biocompatible and degradable [62]. To separate these microfibers and nanofibers from cellulose, a sonication treatment as intensive as ultrasound is crucial. Ultrasound generates a forceful mechanical oscillating power at a high intensity, producing a collapse of bubbles in a liquid, and breaking the intermolecular hydrogen bonding within its structure. Microbubbles will

Table 1
The main parameters, modified materials and the application fields of ultrasound.[a]

Field	Goal	Application	Frequency/kHz	Power/W	Reference
Biology	PGA, PLLA, PDLLG	Tissue engineering	2×10^4	–	[50]
	PLLA, PLGA	Biodegradable polymer coating	–	0.75	[127,128]
	Hovenia polysaccharide	Natural antioxidants	40	–	[56]
	Olive oil	Drug delivery vehicle	20	–	[129]
	CMC, CHI	Regenerating cartilage tissue	20	37	[125]
	Banana peel	Composites intensifier	25	400/800/1000	[130]
	SF, CS	Hydrogels	–/70–1022	–/500/50	[69,70,84,131,132]
	CS	Improve free radical activity	24	100	[133,134]
	SF, wool keratin	Medical instruments	20	750	[67]
	PLA	Tissue engineering	40	150–750	[82,135]
	α-Chitin	Vitamins	–	600	[136]
	Spider silk	Tissue engineering	24	400	[71]
	SF	Tissue engineering	–/24/30/19.8	100–800	[81,84,85,95,117]
	Encapsulated cellulose	Functional materials	–	450	[137]
	Chitosan, betulin, sweet potato pectin curdlan, glucose	Medical materials	20	35/200/130/600	[68,114,138,139]
	Nanoclay	Platelet release	–/40	–	[51,140]
	α-Chitin	Tissue scaffold	60	300	[75]
	Myofibrillar protein, egg white, CHI, ALG	Food engineering	28	100–400	[59,86,96]
	Hyaluronic acid	Functional food	25	50	[109]
	SF	Dental field	50	50	[121]
	PGA, PLGA	Medical textiles	40	250	[124]
Energy	L1, L2, Wood	Renewable energy	20	600	[35,76]
	Miscanthus	Solid fuel	20	500	[74]
	LDPE, HPAM	Petroleum industry.	18–25	50–150	[105–106]
	Fir	Biomass fuel	25–59	240	[37]
	Citrus pectin, lactose	Food industry	20/22	600/–	[31,33,141,142]
	PG, GT	Fossil fuel	20	800	[112]
Environmental	Poplar	Filter media	20–25	400/800/1000/1200	[143]
	PPM	Waste water treatment	–	360–1260	[83]
	Apocynum	Biomass fiber	28	800	[144]
	Starch, polysaccharide solution	Food industry	183/143/99/44/20	100/50	[89,111]
	AAP	Plant protection	20	500	[145]
	Cotton, wool, poplar, red cabbage	Natural dyes	20/28/–	0–500	[12,34,55]
	Cyanobacteria	Inhibit bacterial growth	20/200	20–80	[32]
	BC-NC	Control the degradation of bacterial cellulose	20	100	[108]
	Corn, wheat, potato starch, α-chitin	Food engineering	20/–	170–900	[53,110,113,136,146,147]
	Banana fiber, resin	Mechanical engineering	–	–	[118]
	TPS, NFC, tapioca starch, oil palm fruit	Bioplastics	40/20	250–420	[99,116,148]
	Sisal fiber	Transportation industry	–	–	[123]
	Biconical dihydrazine derivative oxalyl acid	Shape memory material	40	100	[65]
	α-Chitin	Film and flexible foam	60	300	[75]
	Natural rubber, oxalic acid, potato	Wastewater treatment	–/40	–/70–140	[30,66,149]
	Chitin, chitosan	Antibacterial fabric	20/–	100/250	[115]
	Wood, bamboo, wheat straw	Transparent film	20–25	1000	[150]
	Wheatgrass	Available biomass	–	650	[94]
	Ramie	Synthetic fiber	22	400	[151]
Package	Thermoplastic starch, BBE	Antibacterial packaging materials	22.4	300	[122,134]
	Nanocrystalline Cellulose	Drug packaging	–	–	[93]
	D-limonene fiber	Antibacterial film	–	–	[119]
	EVA, Potato starch	Food packaging	20/–	400/–	[100,152]
	SF	Cell encapsulation	–	90	[153]
	TES	Antibacterial material	20/40	400/50	[120,154]
	PVA	Biodegradable plastic	53	–	[43]
	SA, APPS	Fresh-keeping film	40	50	[101]
	Tapioca starch, water hyacinth fiber, corn starch, potato, sweet lime pulp, lotus seed starch, curcumin	Degradable plastic wrap	40/–/40/25	50–1000	[38,102,126,155,156]

[a] Abbreviation: PGA, polyglycolic acid; PLLA, L-lactic acid; PVA, Chlorellapolyvinyl alcohol; PDLLG, polyglycolide; LDPE, low-density polyethylene ; HPAM, Hydrolyzed polyacrylamide; PLGA, copolymer of polylactic acid (PLA) and polyglycolic acid (PGA); CMC, carboxymethyl cellulose; CHI/CS, chitosan; ALG, Sodium alginate; CG, carrageenan; PPM, polypropylene membrane; PROT, protamine; CIP, chitosan-isoleucine-polyethylene glycol methyl ether; SF, silk fibroin; Wool Keratin, wool keratin; L1, wheat straw lignin; L2, Sarkanda grass and wood Quality; PG, Persian gum; GT, western yellow gum; AAP, black fungus polysaccharide; EVA, ethylene-vinyl acetate;; TES, tea polyphenols; BBE, birch bark extract Material; BC-NC, bacterial cellulose nanocrystals; HA, hydroxyapatite; TPS, thermoplastic starch; NFC, water hyacinth fiber; SA, sodium alginate; APPS, apple polyphenols. Symbol '–' represents no relevant parameters involved.

propagate and collapse rapidly, eroding the surface of the material involved, causing a fibrillation of nanofibers or the formation of cellulose nanocrystals [63,64]. Ultrasound was also found to be effective against spider silk fibers [71], chitin fibers [67], collagen fibers and nanofibers [67,68], cotton, bamboo, and ramie fibers in water [69]. Li et al. [72] combined solvent swelling and ultrasound to peel off polyimide fibers. In the process of ultrasound, a rupture of water bubbles formed between fibers causing an increase in the temperature and

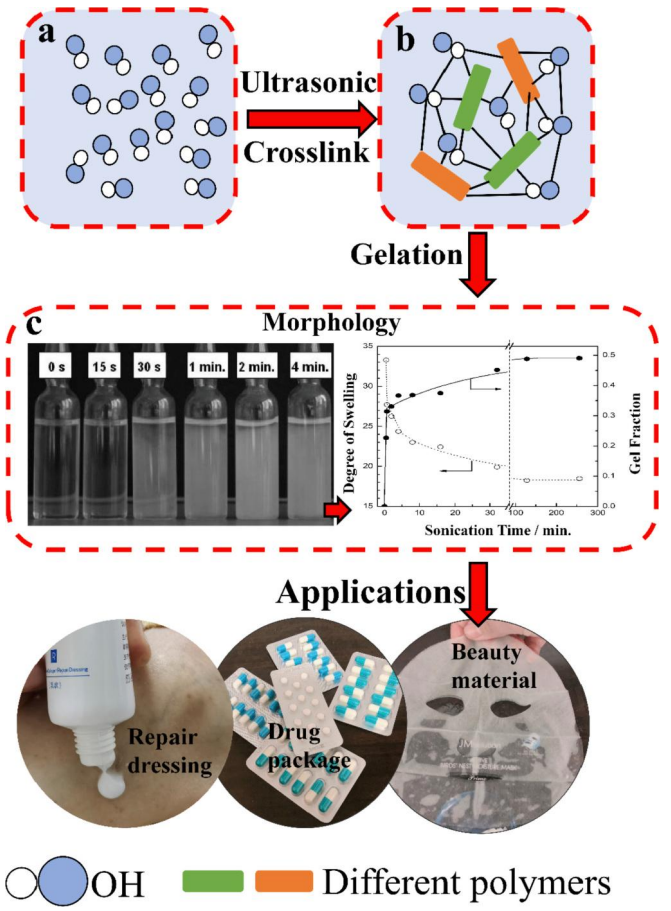

Fig. 3. A scheme of ultrasound-induced crosslinking in biopolymer materials. The cross-linking mechanism of (a) the biopolymer chain in the aqueous solution covalently linking to form (b) a three-dimensional network, in which the polymerization and crosslinking of the bifunctional monomers are mainly caused by the OH radicals initiated by ultrasound; (c) the gel of polyethylene glycol diacrylate (PEGDA 700) formation process at different ultrasonic times, including corresponding applications in skin repair, drug package, and beauty materials. (c) is reprinted with permission from Ref [69]; copyrights (2009) ACS.

pressure. Consequently, the interaction between the fibrils weakens leading to a decreased diameter of the fibers, thus producing the nanofiber. This result ultimately depicts how ultrasound can produce biological nanofibers that consist of a uniform diameter.

Other studies implemented strong bases such as NaOH and KOH to bleach the hemp fibers. This was followed by ultrasound, where the hemp fibers were separated from the ramie [71], and the yield of undecomposed wool, microkeratin and nanokeratin were observed at different treatment time under 300 W ultrasonic power. When the treatment time reached 6 h, the yield increased from 10% to 30%. Wang et al. [73] pointed out that through esterification modification and 100–500 W power ultrasound, the diameter of the original chitin fiber changed from 88 nm to 1662 nm. The esterified chitin fibrils without ultrasonic treatment showed chitin nanofibers with a diameter of about 18–333 nm. In addition, the average diameter of the fibers decreased with the increase of ultrasonic treatment time and power. Singh et al. [74] explored the possibility of ultrasonic assisted alkaline hydrolysis of urea (UAAU) for the pretreatment of miscanthus biomass for delignification. The delignification effect was found to be directly proportional the increasing ultrasound time and NaOH concentration. When the solution consisted of 2.1% NaOH and 1.7% urea at an ultrasound time of 15.5 min, the cellulose and lignin content increased from 43.0% and 23.25% to 47.8% and 27.5%, respectively. In a study on ultrasonic chemical extraction, Lu et al. [75] treated microscale fibers at 300 W high intensity ultrasound. The study resulted in a decomposition of the microscale fibers into water nanofibers. Ultrasound was performed under alternating intensities, producing cavitation that caused shock waves, destroying hydrogen bonds and van der Waals forces. Chitin gel rapidly broke into small pieces, forming nanoparticles that self-assembled to form chitin nanofibers. Nanofibers prepared by ultrasonic treatment can be easily constructed with porous membranes that have been found to possess excellent mechanical properties, consist of smaller fibers, have higher contact surface area, and lower densities [72]. Gilca et al. [76] also reported that the use of ultrasound can cause the rupture of macromolecular chains, improve the extraction rate and purity of lignin, and physically modify lignin under 600 W ultrasonic power, successfully obtaining nanoparticles. Therefore, ultrasound technology has become a convenient, versatile and environmentally friendly manufacturing method for extracting bio-nano fibers and particles from natural products [77].

Several studies touch on the application ability of ultrasound to improve the movement and synergy of molecules, thereby affecting the physical and chemical properties of polymers. Ultrasonic action can promote the graft polymerization of acrylic acid into polypropylene fiber membranes, improving the overall structure. In a study performed to promote the grafting of acrylic acid polymerization into a polypropylene fiber membrane, ultrasonic action was implemented to enhance its structure [83]. The graft polymerization was measured to be from 0.18 mg/cm^2 up to 0.86 mg/cm^2 at a power of 1080 W. The study found that the product exhibited outstanding hydrophilicity as well as great anti-scaling performance due to the formation of hydrophilic groups generated between them [83]. Moreover, natural polymer materials, such as silk, have unique physical and chemical properties along with excellent biocompatibility properties [78–80]. Ultrasound technology can modify the enzymatic degradation, as well as alter the chemical and mechanical properties of silk [81]. One study applied ultrasound to silk fibroin in aqueous solution to evaluate the effect of ultrasound on its molecular weight, its solvent to gel transition behavior, and its physical and chemical properties [81]. By increasing the ultrasonic power to 750 W, researchers found that the morphological structure of polylactic acid foam changed to form large 3D holes, displaying several desirable mechanical properties.

Although ultrasonic treatment did reduce the molecular weight of the silk fibroin solution, some studies have pointed out that the free radical cross-linking reaction caused by ultrasound is common in the degradation process [60]. This led to the creation of the ultrasound-induced protein polymer gels. When the silk fibroin self-assembled into a silk fibroin gel network under ultrasound, it can transform from a solution state to a hydrogel state, forming a β-sheet-rich conformation. This result was confirmed in a study on recycled silk fibroin film by Susanin et al. [84]. Another study found that when ultrasound time reached 2 h, the α-helical content (Fig. 4a) reached its maximum (Fig. 4b). As the ultrasound time increased, the water molecules and silk fibroin molecules in the solution accelerated via ultrasonic treatment, and the β-sheet structure steadily increased [82]. In Fig. 4c, the maximum β-sheet content was reached at 4 h. The results of this study were confirmed by Carissimi et al. [85] in a comparison study on the effects of different silk degumming methods on the silk structure. Although the results were confirmed, the β-turn in the structure still accounts for 20% of the total silk secondary structures after ultrasound. The researchers in this study suggested that this is due to a decline in the repulsion between the silk fibroin molecules caused by ultrasound. The interactions between the chains were reduced, and the β-turn content in the silk fibroin molecules remained unchanged or increased. Li et al. [86] found that in the strong ultrasonic field, the aggregation distance between adjacent myofibrillar proteins can be reduced and the protein structure can be stabilized from ultrasound-induced re-aggregation. This can help to increase the number of hydrogen bonds and promote the transformation of β-turn and random coil structures to β-sheet structure.

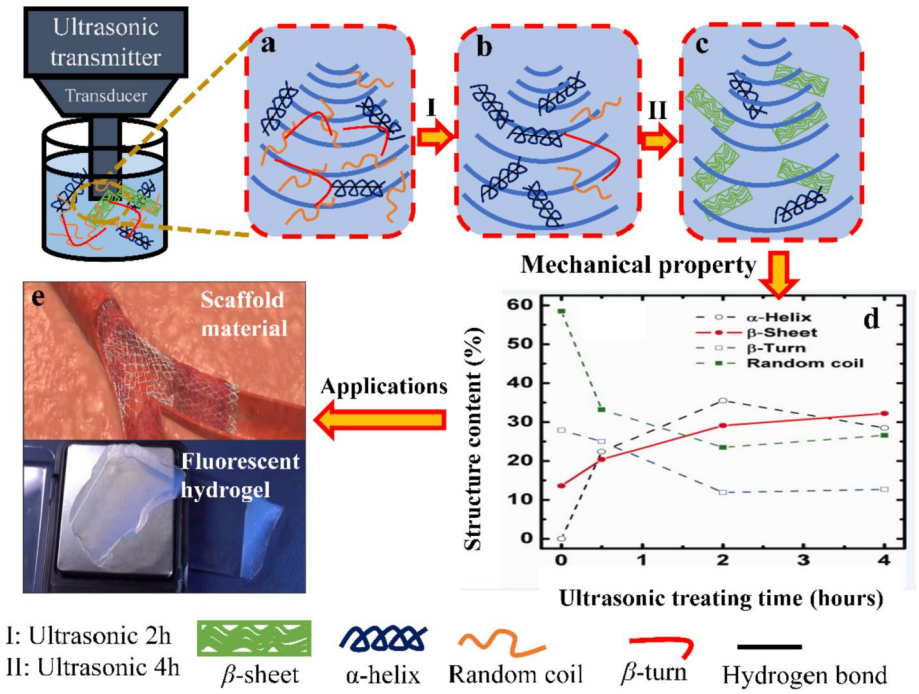

Fig. 4. A schematic diagram of the ultrasonic effects on silk fibroin proteins. A newly prepared silk fibroin solution displays (a) a typical random coil conformation and becomes (b) dominant α-helix conformation after 2 h of ultrasound, then (c) the β-sheet conformation content in silk fibroin solution reaches 32.2% after 4 h of ultrasound, and (d) the secondary structure contents changes with ultrasound time. (e) Their potential applications in tissue scaffolds and fluorescent hydrogels. (d) is reprinted with permission from Ref [95]; copyrights (2007) Wiley.

Furthermore, polymeric materials consist of crystal structures and unique orientations that are closely related to the physical and mechanical properties of the molecules involved [87]. For example, the untreated SF containing amorphous materials undergo rapid degradation than that of crystalline cellulose materials treated by ultrasound [87]. Ultrasonic crystallization is commonly used in crystal nucleation with power ultrasound, which can be used to manipulate the crystallization process [86]. In solution, ultrasound produces cavitation bubbles that generate high pressures and temperatures. These cavitation points are considered to be preferential nucleation centers, and lower critical energy generates crystal formation. Simultaneously, sound waves can stimulate contact and mass transfer between molecules, promoting crystal nucleation [87].

A study of cellulose under ultrasound was conducted in a system of HCl-$FeCl_3$ [88]. Through the study, it was found that ultrasonic treatment can cause fiber cavitation, as well as affect the morphology and microstructure of the cellulose fiber. Ultrasonic treatment was found to enhance the reaction of chemical solvents to the loose amorphous region of cellulose. The acid hydrolysis of the plain amorphous region increased the crystallinity, but it did not change the chemical structure of cellulose. Another study by Tischer et al. [88] proved that ultrasonic treatment can effectively change the micro-fibrillated structure of cellulose and increase the average grain size and crystallinity of the material. A study by Andrade et al. [89] implemented high-intensity ultrasound for the extraction of starch nanoparticles from breadfruit. It was shown that after 75 min of ultrasonic treatment, ultrasonic cavitation caused rupturing of the crystal area of the nanoparticles and the formation of amorphous particles. Zheng et al. [90] used 25 and 80 kHz single and dual frequency under 720 W ultrasonic power to study the structure and performance of sweet potato starch, and also found that the crystal structure was damaged and the amorphous structure increased. Compared with single-frequency ultrasonic treatment, dual-frequency ultrasonic treatment has more obvious damage to the crystal structure of starch suspension. Minakawa et al. [91] found that using 20 kHz ultrasound for 30 min at room temperature (25 °C) will strongly affect the crystal structure of starch, and the ultrasound affects the arrangement of the double-helix chain that forms the crystalline component in the starch, which will lead to starch crystallinity to be reduced or completely amorphous. The new structures were orderly arranged into biopolymer chains, forming a network that can effectively diffuse water, and increasing the stiffness of the biopolymer matrix, suggesting that it could be considered as a suitable plasticizer. In addition, low crystallinity is very important for the application of materials as carriers for compounds (such as drugs in drug delivery systems) [92].

Nanocrystalline cellulose samples were obtained by hydrolyzing microcrystalline cellulose with ionic liquids in a study by Ishak et al. [93]. This study led to the discovery that with a longer ultrasound time, the weaker the crystallization. For example, when ultrasound was applied for 5 min, the crystallinity index increased from 60% to 73%. However, as the ultrasound time increased to 20 min, the crystallinity index declined from 73% to 65%. Therefore, under an ultrasonic time of 5 min, ultrasonic treatment can effectively act on the amorphous area and increase the crystalline content. When the ultrasonic time reaches its limit, the ultrasound acts on both the amorphous region and crystalline region simultaneously, causing the crystallinity of the material to decline. Additionally, the breakage of intermolecular hydrogen bonds between the nanocrystalline cellulose molecules through the ultrasonic cavitation result in a crystal structure collapse, ultimately leading to a lower crystallinity. Another study was conducted using wheat straw by Qu et al. [94]. This group found that the crystallinity of the material increased by 12.48% after 35 min of ultrasound. During ultrasound, the potential energy of the expanding bubble transformed into kinetic energy under ultrasonic cavitation. The liquid jet passed through the bubble at a speed of several hundred meters per second and hit the surface of the wheat straw, creating an active surface. The cell wall of the wheatgrass structure was then weakened, causing a removal of the amorphous phase and producing higher crystallinity. These studies together provide a guideline for the preparation of higher crystallinity materials using ultrasound with a more in-depth study of the internal changes that can occur within biopolymer materials [89].

4.2. *Causes of reunion*

Nanoparticles of polymer materials can easily form agglomerates during the composite process. Compared with traditional methods such as mechanical stirring, ultrasound can extensively control the particle sizes along with the uniformity of the agglomerates that form. The high energy produced by cavitation increases the particle interaction in the

suspension, leading to smaller agglomerate sizes within the processed composites. The momentum of the solid powder suspended in the fluid near the cavitation bubble may increase, which may cause ruptures during collision, resulting in a decrease in their average particle size [20].

Based on this information, ultrasound can be used to manipulate the required average particle size and control the particle size distribution, aggregation morphology, and intermolecular interactions [93]. One study [96] found that after ultrasonic treatment of chitosan-sodium alginate at a frequency of 28 kHz for 10 min, the particle size of the polymer decreased to about 10 nm. At a higher frequency with a lengthened treatment time, such as 40 kHz for 30 min, the particle size was found to increase to 50 nm. The researchers found that the shearing effect during ultrasonic cavitation induced a fracture in the chemical bonds of the macromolecules, as well as molecular degradation, expansion, and an overall structural rearrangement of the polymer. Another study confirmed the idea that ultrasound can uniformly distribute particles within the polymer matrix, proving ultrasound an effective method to destroy agglomerations [95]. In addition, several studies found that ultrasound can break larger lysozyme microspheres. One study used 213 kHz ultrasound to reduce the size of lysozyme microspheres from 0.5–4 lm to 0.5–2 lm [96], there are also studies [97] that explored the mechanism of ultrasound to promote enzymatic reactions. Treatment under different conditions of 35–75 °C (especially above 65 °C), 90–360 W and 10–50 min, will cause enzyme inactivation. Ultrasound could also cause pores and cracks on the surface of starch granules: Zheng et al. [90] pointed out that more dents and holes appeared on the surface of starch granules after 720 W ultrasonic treatment; Sujka et al. [98] also found that after using 170 W ultrasonic treatment in water, small cracks and depressions appeared on the surface of starch granules, generating free radicals along the way that will cause the molecular chains of starch to break [97]. Several aspects of the biopolymer can be arbitrarily altered, such as particle shape and size along with the aggregation morphology and the surface properties of the polymer [98]. In a study where ultrasound was applied to agglomerated nano-A_2O_3 particles in epoxy resin, cavitation destroyed the strong agglomeration present within the nanoparticles, transforming the nanoparticles into an even distribution within the composite material [98].

A study by Asrofi et al. [99] involved the preparation of nanocellulose by using water hyacinth as a raw material. It was discovered that the released kinetic energy caused an even distribution of the fiber's matrix, destroying any fibrous clumps present. In a related study, Anayansi et al. [100] proved that ultrasound generated an entirely uniform dispersion of titanium dioxide nanoparticles within the ethylene-vinyl acetate copolymer matrix, which could be useful in the enhancement of antibacterial properties [95].

Ultrasound can also increase the degree of mixing in active crystals [101]. Additionally, it can produce an increase in the number of particles and in the collision frequency for an even dispersion of the crystals within a solution before the formation of agglomerates. A mechanism of this is shown in Fig. 5a, b. Fig. 5c presents the scanning electron microscopy (SEM) observation of the freeze-dried the crystallized particles of active pharmaceutical ingredients denatured with methyl ethyl keton (MEK). It can be noted that the material displayed better dispersibility after 300 min of ultrasound, as compared to the SEM image after just 3 min.

An important effect that can occur through ultrasound is the phenomenon of reunion. This can be explained by ultrasound time adjustments that may contribute to the formation of varying cluster sizes within nanofluids. For instance, if the ultrasonic time increased from 10 min to 60 min, the size of the nanoclusters will gradually decrease.

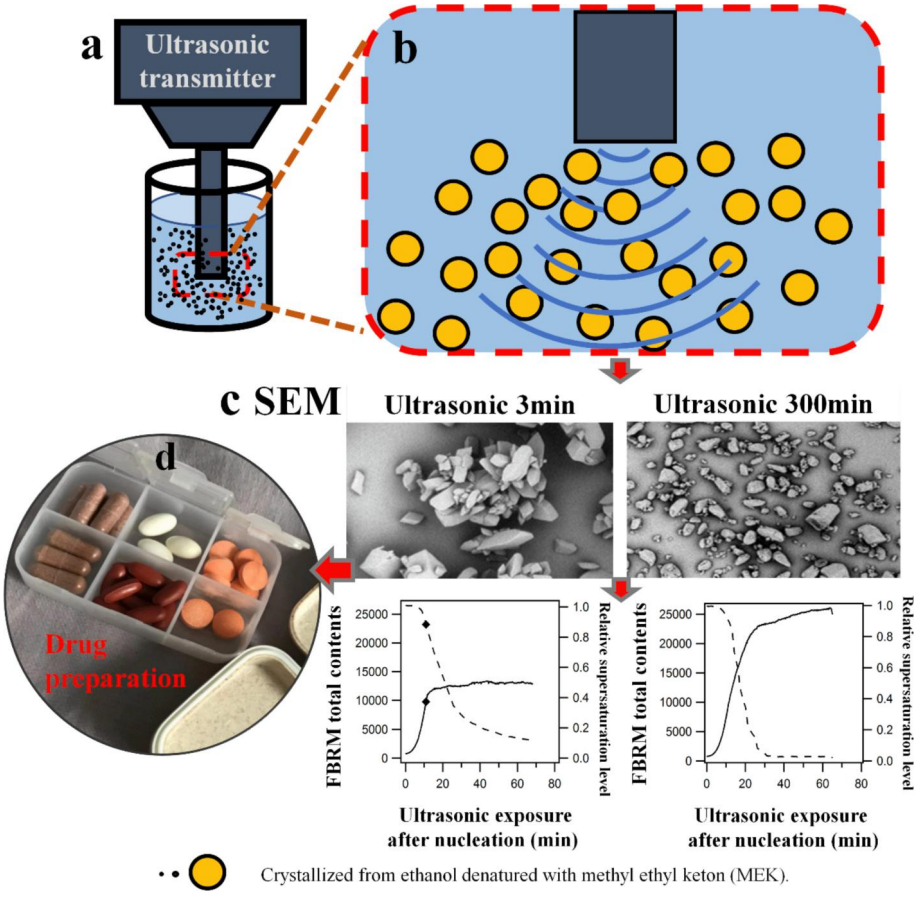

Fig. 5. A schematic diagram of particle changes during ultrasound treatment. (a) The biopolymer particles were ultrasonically treated in a solution (an enlarged view is presented in (b)); (c) the crystallized particles of active pharmaceutical ingredients denatured with methyl ethyl keton (MEK) changes were tracked under different ultrasonic time (3 min and 30 min by SEM images), using the Focused Beam Reflectance Measurement (FBRM) technology. (d) Corresponding applications in the drug preparation industry. (c) is reprinted with permission from Ref [104]; copyrights (2017) MDPI.

However, if the ultrasonic time exceeds the optimal value for that material, the cluster size will increase once again [102]. This idea was exhibited in an experiment by Lan et al. [101], where the effect of different ultrasound times was studied on sodium alginate (SA), apple polyphenol (APP), and silver nanoparticle composite films. The results of this study suggested that the reduced distance between the particles caused the aggregation factor and dispersion factor to decline, leading to agglomeration. This effect led to an inhomogeneity in the structure of the material, significantly reducing the tensile strength of the composite films in the study. As the ultrasound time reached 30 min, the particle aggregates were decomposed into smaller particles, increasing the tensile strength. However, when the ultrasonic treatment time exceeded 40 min, the dense and uniform network structure of the composite films were disturbed, causing the nanoparticles to aggregate once more.

An additional aspect to note is that of the hardness value of nanoclay/epoxy resin nanocomposites at different ultrasonic times. When the ultrasonic time reached 10 min, the diameter size of the nanoclay clusters decreased, and the surface area for the interaction with the epoxy resin increased, causing an increase of the overall hardness of the material. After the ultrasound time exceeded its threshold for that material, the size of the nanoclay clusters increased again, and the distance between those clusters increased, which resulted in an undesirable decline in the overall mechanical properties of the material [104]. Lin et al. [102] utilized different ultrasonic powers of 200 W, 600 W and 1000 W at different ultrasonic times of 5 min, 15 min, and 25 min to manipulate lotus seed starch nanoparticles. A buffer solution was used to assist in the enzymatic hydrolysis for the preparation of starch nanoparticles. With the increase of ultrasonic power and time, the starch nanoparticle sizes gradually decreased from 334.7 nm to 123.33 nm. This relation is due to an escalated ultrasonic intensity, which weakened the interaction between the starch molecules. A more concentrated distribution of the starch molecular chains then occurred. It was found that when the power and time continued to increase, the particle size did not. The researchers in this study theorized that this is due to the smaller particles adhering to the large particles, agglomerating into larger masses. Similarly, Jambrak et al. [103] used 100, 300, and 400 W ultrasonic powers to sonicate corn starch at 15 and 30 min and found that the use of 100 and 300 W ultrasonic power had the greatest impact on the particle size and its reduction. When energy was applied to 400 W, starch granules tended to agglomerate. Vallejo-Domínguez et al. [62] observed that under the action of ultrasound, the polymer particles appeared dense and multi-layered. As time increased, the surface of the polymer corroded. After 35 min of sonication, more dense particles were observed. These studies prove that a precise selection of the ultrasound time and power are both critical in ultrasound treatment of biopolymer materials.

4.3. Degradation of macromolecules via ultrasound

Ultrasound technology involves hydrodynamic forces that influence a decomposition reaction in macromolecules. This can be explained by the breakage of polymer chains during ultrasound, where the samples produce fragments of a selected molecular size. This is where ultrasound technology can be easily distinguished from chemical or thermal decomposition reactions since ultrasonic degradation is non-random [106]. A temperature change occurs that leads to a rapid degradation of larger molecules while the molecular weight of the polymers decreases [107,108]. Findings in several studies were consistent with the idea that ultrasound is efficient to reduce the molecular weight of macromolecules. For example, it was found that increasing ultrasonic intensity caused the average molecular weight (M_w) of low-density polyethylene (LDPE) to decrease from 19.45×10^4 g/mol at 0 W to 12.91×10^4 g/mol at 150 W [105]. LDPE was found to degrade by 50% under ultrasonic action at 60 °C with a power of 240 W, while the degradation rate dropped to 30% at 80 °C. The results of this study suggested that the cavitation effect could be enhanced at lower temperatures, leading to higher degrees of degradation [106]. Additionally, in a hydrolysis experiment of polyacrylamide, the viscosity of the solution sample decreased from 65 MPa-s under 18 kHz ultrasonic frequency to 3.4 MPa-s under 20 kHz frequency, suggesting a higher degree of degradation due to a higher ultrasonic frequency [107].

In the field of biochemistry, ultrasound is typically used to break down cells and components in living tissues, in order to effectively extract its soluble constitutes. In a study by Wardhono et al. [108], it was found that ultrasonic cavitation is the cause of cellulose degradation. This study was performed under 100 W ultrasound in a water/ethanol solution. In an additional study, ultrasound was implemented to extract hyaluronic acid. Hafsa et al. [109] found that free radicals cleaved the glycosidic bond between gluconic acid and acetamido formamide, obtaining a lower molecular weight of hyaluronic acid. Hafsa et al. [109] also believe that 50 W ultrasound will also induce a significant decrease in the average molecular weight of hyaluronic acid. The same research team [97] pointed out that 40 min of ultrasound time and 360 W of ultrasound power will destroy the hydrogen bonds of starch, destroy the starch chain, and significantly reduce its molecular weight.

Materials such as starch, sweet potato flour, and chitosan all have high molecular weights along with low mechanical strengths [109–111]. For example, Boufi et al. [110] performed an ultrasound study on starch, where after 15 min of ultrasound at 10 °C with an ultrasonic power of 400 W, the particle size decreased from 1000 nm to 600 nm. After 75 min, the particles reached about 85 nm, and the particles size was found to stabilize at around 40 nm. The idea that ultrasonic cavitation reduces the molecular weight of starch was further explored by Yasuo et al. [111], where it was also proved that ultrasound cavitation significantly decreases the viscosity of starch.

In an additional study, chitosan was modified with 3,4-dihydroxybenzoyl (CS-DHBA) and 3,4,5-trihydroxybenzoyl (CS-THBA) in 1% acetic acid solution. In this particular study, the molecular weight decrease was consistent with those present in literature, although the decrease was not as profound. The minimal change in molecular weight could be due to the flexibility of the chitosan molecules. After modification, the flexibility increased, and the shear force of the cavitation field was not strong enough break down its bonding [116].

Ultrasound plays an important role in the degradation of pectin, polysaccharide and resin. Raoufi et al. [112] performed ultrasonic modification on two native Iranian gum exudates, Persian gum (PG) and Western yellow gum (GT). The gels in this study are water insoluble, due to the heterogenous polymer polysaccharides composed in the gel structures. Due to these factors, the applications of these materials in the food and pharmaceutical industries are limited. The study involved a 20 kHz sonication that produced a breakage of the molecular skeleton or side branches, resulting in structural conformation changes that decreased the viscosity of the materials. A larger substance will gradually decrease in molecular mass as its time under ultrasonic treatment increases, leading to a narrower molecular weight distribution. This is due to a longer relaxation time exhibited within larger molecules when exposed to an ultrasonic field, as these molecules are not easily resistant against ultrasonic stress [109].

Similar studies suggested the ultrasonic reduction of the molecular weight of pectin occurred though an irregular shearing of the side chains within the molecule. Simultaneously, an escalation of ultrasonic power and time caused its decomposition, generating lower molecular weight fragments of the molecule [119]. In another study, ultrasonic treatment of the black fungus polysaccharide caused the molecular weight and viscosity to reduce, as its rheology and antioxidant activity improved [120]. Sujka et al. [113] used ultrasonic waves at a frequency of 20 kHz and power of 170 W to treat rice, corn, wheat, and potato starch granules. The results presented in this study showed that shock waves formed through the collapse of the bubbles, causing high-speed collisions within the particles.

Cheung et al. [114] conducted an ultrasonic study using 0.1 M and 0.3 M sodium hydroxide solutions with β-glucan. The high-intensity

ultrasound was found to promote the degradation of β-glucan, as the polysaccharide degraded from its original triple-helical structure to one that is double-stranded (Fig. 6a). The structure then transformed into a random coil structure (Fig. 6b). As the ultrasonic time lengthened, the intrinsic viscosity decreased. The curdlan chain had a helical conformation in 0.1 M sodium hydroxide, but it shifted to a random coil structure in 0.3 M sodium hydroxide. The degradation rate in 0.3 M was much higher than the degradation rate that was present in the 0.1 M sodium hydroxide solution. The researchers in this study suggested this relationship is due to the random coil confirmation present in the gels are more prone to degradation than the gels with a helical conformation. Additionally, as the alkali concentration increased, the intramolecular and intermolecular hydrogen bonding between the main chains become fragile, leaving the random coil conformations susceptible degradation. Another study was conducted on α-chitin using ultrasound [103]. The results presented in this study found that the stronger intermolecular forces present in the molecular structure prevented ultrasound alone from directly dispersing α-chitin. This study was altered by performing the ultrasound weak, acidic conditions. With increasing ultrasound time, smaller chitin particles were generated and the emulsification of α-chitin was greater. Zou et al. [115] tested the dispersion of chitin under different ultrasound times from 0 to 270 min. The results show that 100 W ultrasonic power can successfully prepare a single chitin nanofiber. After 150 min of treatment, it showed cross-linking, crimping and clear small fibers with a width of about 300 nm. With the progress of ultrasonic treatment, the agglomeration was broken down into irregularly shaped individual nanofibers with a width of 9–120 nm. Other studies [87] also discovered that 1000 W high-intensity ultrasound can be well applied to the separation of natural fibers. Ultrasonic impact can gradually disintegrate the complex multilayer structure and separate cellulose fibrils from amorphous materials. The resulting materials were stable after long-term storage. The results of this study suggested a method preparing dispersed α-chitin with excellent emulsifying ability. This method could be further extended to water-soluble polysaccharides and cellulose, making it play important potential applications in plant protection, antibacterial, anti-cancer, packaging, and prebiotics.

4.4. Improvement of mechanical properties via ultrasound

Select studies have implemented ultrasound technology for the investigation on the mechanical properties of different biopolymers [40]. One study by Suryanto et al. [116] incorporated nanoclay to the matrix and found that the performance of the biocomposite material was increased, although it was difficult to create the biocomposite matrix

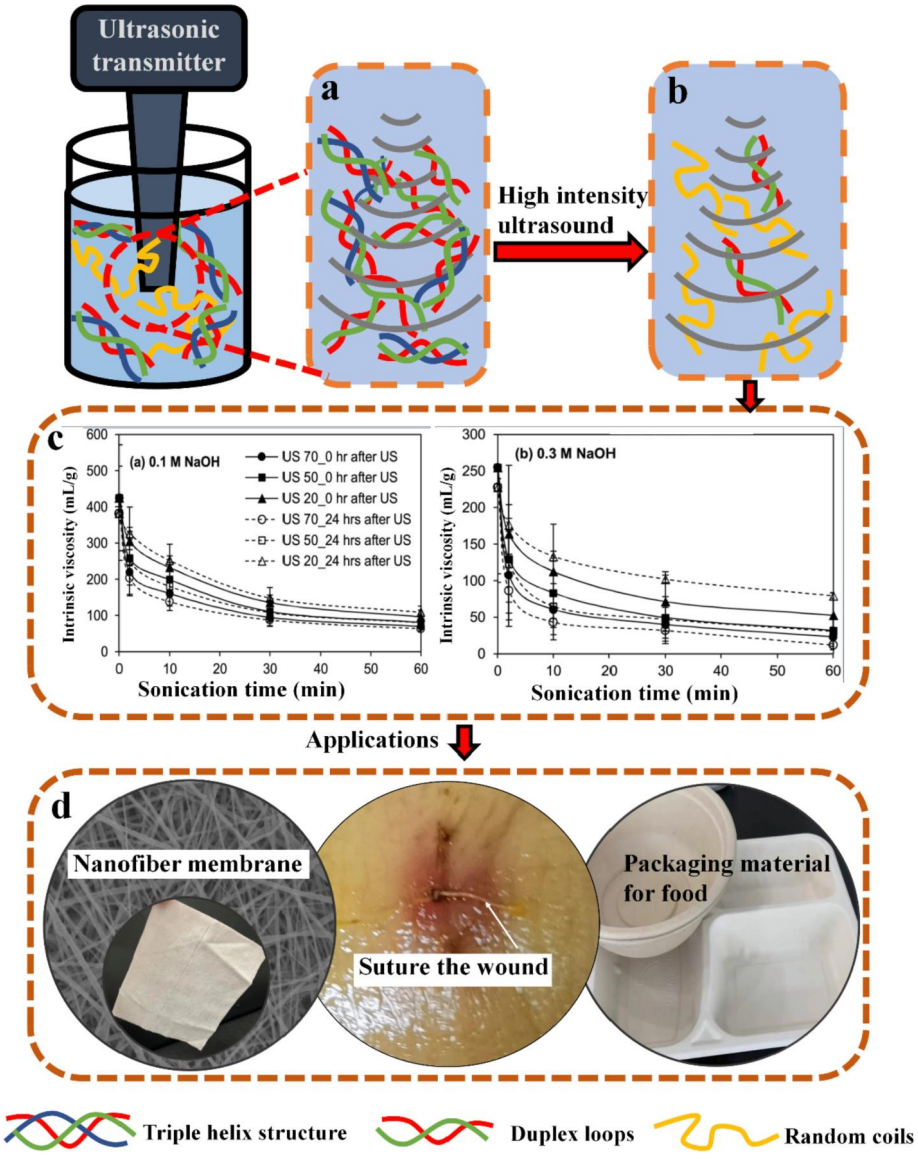

Fig. 6. A schematic diagram of β-glucan under ultrasonic modification. The chain conformation of β-glucan was degraded from (a) triple-helix structures to (b) duplex loops and random coils; (c) after ultrasonic treatments with different intensities and times, the viscosity of gelatin polysaccharide solution decreased in 0.1 M and 0.3 M alkaline solutions, respectively. (d) Nanofiber membranes, wound sutures and food packaging materials are potential applications of this ultrasound technology. (c) is reprinted with permission from Ref [114]; copyrights (2018) Elsevier.

that consisted of homogenous nanoclay particles. The starch-based composite material was subjected to ultrasonic treatment for the homogenization of the nanoclay particles and for the overall enhancement of the mechanical properties of the material. The 5% nanoclay material was ultrasonically treated for 15, 30, 45 and 50 min. It was found that the longer the treatment time, the more uniform the nanoclay particles were dispersed in the solvent or starch matrix, thus improving the properties of nanoclay starch. An additional study was performed to test the strength of the composite materials, and it was found that the mechanical strength of the composite materials increased from 11.79 MPa to 28.01 MPa. A study by Cai et al. [117] treated a silk fibroin solution in formic acid with an increasing ultrasonic power. The results of this study demonstrated that ultrasound could promote the self-assembly of regenerated silk molecules, enhance the interaction between calcium ions and silk molecular chains, and increase the elastic modulus of silk fibroin membrane. As the ultrasonic intensity increased, the elastic modulus of the films increased from 0.08 ± 1.21 MPa (at 100 W) to 9.13 ± 0.31 MPa (at 800 W), suggesting that the ultrasound treated materials possessed good mechanical strength and flexibility.

Ghosh et al. [118] found that the ultrasonically treated samples showed good resin permeability. This indicates that ultrasound promoted a strong bonding force between the fiber and the resin. It was found that ultrasound treatment pairs well with the wood chemical treatment technique, as this combination of treatments can improve the mechanical properties of composite materials more effectively than by just using the chemical treatment alone [141]. Additionally, ultrasonic treatment has been found to significantly increase the tensile strength value of corn starch/stearic acids/odium carboxymethyl cellulose composite films. This is due to the shockwave and mechanical force that occurs during ultrasound treatment that promotes the interaction of larger molecules between the film-forming components [126].

Some studies discovered that an increase in ultrasonic treatment time causes the tensile strength of the material to decrease. This was recently found in a study on the tensile strength of the antimicrobial active packaging fiber polyvinyl alcohol/D-limonene. When the ultrasonic treatment time increased to 15 min, the tensile strength increased from 3 MPa to 4 MPa. After the ultrasonic treatment time exceeded the 15-min marker, the tensile strength decreased to 3.7 MPa [119]. The same study found that ultrasound destroys the relationship between the tea polyphenol and the polyvinyl alcohol molecules. The hydrogen bond present within the molecules reduces the intermolecular force. However, the mechanical properties of the composite membrane were improved with an extended ultrasonic treatment time. At this time, the hypermixing effect was found to lead the molecules to rearrange to form a denser and more uniform network structure [120].

Serôdio et al. [121] combined ultrasound with a well-known technique known as electrospinning. The two methods were implemented to prepare silk fibroin (SF)/polyoxymethylene (PEO) membranes. It was suggested that ultrasound can adjust the viscosity of the solution and induce water stability in the electrospinning matrix. In samples consisting of 10% SF: 20% PEO, the tensile strength increased from 1.19 MPa to 2.84 MPa as the ultrasonic time increased from 0 to 20 min. As the content of birch bark extract in the material composition increased, ultrasonic treatment can increase the fracture stress of the mixture of starch and birch bark extract [122].

It was confirmed that ultrasound can eliminate the micro gap at the fiber matrix interface, reducing the porosity of the material, and thus allowing samples to better penetrate and adhere to the fiber. With an improved dispersion of the fiber along the matrix, the tensile strength will drastically improve [131]. In an example from literature, 1 wt% of cellulose nanofiber was extracted from water hyacinth and yam, then sonicated at 49 kHz, at an ultrasonic power of 250 W for 0, 15, 30 and 60 min to prepare a bioplastic. Later, the maximum tensile strength of the nanocomposite increased from 4.0 to 11.4 MPa [99]. When these results were compared with a traditional chemical method separately, the addition of ultrasound increased the number of hydroxyl groups on the surface of cellulose in the polypropylene-based wood-plastic composite wood, thereby improving the adhesion between the fiber and the matrix.

Pipathattakul et al. [123] discovered an example of the tensile strength of a material increasing after undergoing surface modification via ultrasound. When sisal fiber was immersed in a sodium hydroxide solution, it was subjected to the high-speed ultrasonic impact jet. This removed any dirt particles along the surface of the fiber, and the continuous ultrasonic jet caused the lignin and cellulose within the sisal fiber to gradually separate. When the ultrasound ran for 90 min, the modified composite material displayed a smaller fiber diameter, and the adhesion to the matrix was strengthened. This led to a tensile strength increase from 13 MPa to 17 MPa.

It was proven by Wang et al. [124] that ultrasonic modification is also effective to improve the tensile properties of polylactic acid-polyglycolic acid (PLGA) fibers. After ultrasonic modification, the fracture strength of the PLGA fibers increased from 7 to 8.5 cN/dtex. The elongation was found to reach up to 28%, much higher than that of the unmodified PLGA fiber. In another study, Belluzo et al. [125] prepared a compatibilized blend of polyelectrolyte complex (PEC) with carboxymethyl cellulose (CMC) and chitosan (CHI) that underwent ultrasound at 20 kHz and 37 W. The study compared the composites with and without ultrasonic treatment. It was found that in the ultrasonic-treated material, the pore structure distribution was more uniform, and the surface and internal structure were stabilized. The mechanical properties increased with the decrease of the pore size. The more uniform the pore size distribution was, the greater the mechanical properties that the materials had. The compressive strength of the composite after ultrasound increased from 155.7 ± 44.1 kPa to 493 ± 117 kPa, and the mechanical properties of PEC were found to significantly improve within the ultrasonic treated material. Asrofi et al. [126] used tapioca starch and 10% water hyacinth fiber to composite. These were treated under 40 kHz, 250 W ultrasonic action for 0, 15, 30 and 60 min. The results indicated that the tensile strength and tensile modulus increased by 83% and 108%, respectively. The team suggested that the reason for this was due to an even dispersion of tapioca starch in the water hyacinth fiber under the action of ultrasound, creating strong hydrogen bonding that made the interface adhesion stronger. Therefore, the above-mentioned studies show that ultrasound can effectively disperse a substance in a uniform manner into another matrix material. A certain interaction will occur between the components, thereby improving the mechanical properties of each composite material studied.

5. Conclusion

This review recounts the basic theory behind ultrasound and reports its related applications. Ultrasound is a method that can be used on its own, or in conjunction with other standard methods for the preparation of new biomedical and sustainable engineering materials. Ultrasound technology has several advantages which include its high efficiency, cleanliness, and reproducibility. In comparison with the traditional physical and chemical methods of material fabrication, ultrasound possesses capabilities to significantly alter the performance and structure of biopolymer materials. Although many researchers have already proven the potential of ultrasound to modify naturally derived materials, this technique is still new to the field of biological and sustainable materials. In this review, we demonstrated that in order to successfully transition ultrasound technique into the bio-/green material field, the community have made tremendous progress in the selected areas.

Although studies have revealed that the effect of cavitation is closely related to the formation of stable cavities, many of the theories and mechanisms behind cavitation are still unknown, as the interaction of heat, machinery, and sound generated during cavitation requires further investigation. Another area of concern would be the issue of expanding ultrasound in scale while conserving its efficiency.

In summary, the current study on ultrasound for the field of

biopolymer materials is still under development. Although ultrasound is widely recognized across the medical and biological community, in recent years, this technology has rapidly emerged for the use of creating and modifying new biopolymer-based materials. This review entails the current development of ultrasound methods used for these materials, establishing that this topic holds a vast potential for the advancement of novel materials.

As research in this field progresses, ultrasound is proving to be an effective preparation method amongst several other universally recognized polymer modification techniques such as plasma sputtering, UV irradiation, grafting, and metallization [128,157–159]. In a more specific bio-tissue engineering application, UV irradiation could be implemented for the surface property modification of biopolymers such as Poly-L-Lactic acid (PLLA) or polymethylpentene [128]. While traditional methods have proven to be effective, the use of ultrasound technology could be a more impactful and cost effective advancement in the field of biomaterials.

Acknowledgements

This study is supported by the National Natural Science Foundation of China (21973045). J.M. and X.H. are supported by Rowan University Seed Research Grants, the US NSF Biomaterials Program (DMR-1809541) and Future Manufacturing Program (CMMI-2037097).

References

[1] T.G. Yashas Gowda, M.R. Sanjay, K. Subrahmanya Bhat, P. Madhu, P. Senthamaraikannan, B. Yogesha, Polymer matrix-natural fiber composites: an overview, cogentEngineering 5 (1) (2018) 1446667.
[2] A. Nuryawan, N.G. Olaiya, P. Kayode Oke, H.P.S. Abdul Khalil, S. Rizal, P. B. Mogaji, E.R. Sadiku, S.R. Suprakas, P. Kayode Farayibi, V. Ojijo, M.T. Paridah, The role of two-step blending in the properties of starch/chitin/polylactic acid biodegradable composites for biomedical applications, Polymers 12 (3) (2020) 592.
[3] J. Agarwal, S. Mohanty, S.K. Nayak, Valorization of pineapple peel waste and sisal fiber: study of cellulose nanocrystals on polypropylene nanocomposites, J. Appl. Polym. Sci. 137 (42) (2020) 49291.
[4] F. Wang, H. Liu, Y.Y. Li, Y.J. Li, Q.Y. Ma, J. Zhang, X. Hu, Tunable biodegradable polylactide-silk fibroin scaffolds fabricated by a solvent-free pressure-controllable foaming technology, ACS Appl. Bio Mater. 3 (12) (2020) 8795–8807.
[5] T.H. Mokhothu, J.M. Jacob, Review on hygroscopic aging of cellulose fibres and their biocomposites, Carbohydr. Polym. 131 (2015) 337–354.
[6] T.E. Nikiforova, V.A. Kozlov, F.Y. Telegin, Chemisorption of copper ions in aqueous acidic solutions by modified chitosan, Mater. Sci. Eng. B 263 (2021), 114778.
[7] A. Iovene, Y.W. Zhao, S. Wang, K. Amoako, Bioactive polymeric materials for the advancement of regenerative medicine, J. Funct. Biomater. 12 (1) (2021) 14.
[8] F. Wang, N. Wolf, E.M. Rocks, T. Vuong, X. Hu, Comparative studies of regenerated water-based Mori, thai, eri, muga and tussah silk fibroin films, J. Therm. Anal. Calorim. 122 (3) (2015) 1069–1076.
[9] K.F. Xie, Y.C. He, Y.H. Wang, D.S. Zhou, W.B. Hu, Characterization of polymer crystallization kinetics via fast-scanning chip-calorimetry, Acta Phys. -Chim. Sin. 36 (6) (2020) 1905081.
[10] E.H. Kim, G.D. Han, S.H. Noh, J.W. Kim, J.G. Lee, Y. Ito, T. Son, Photo-reactive natural polymer derivatives for medical application, J. Ind. Eng. Chem. 54 (2017) 1–13.
[11] C.W. Wong, C.Y. San, J. Jaison, P. Kaushik, B. Mikhael, E.M. Abd, G.S. El-Sayyad, Response surface methodology optimization of mono-dispersed MgO nanoparticles fabricated by ultrasonic-assisted sol-gel method for outstanding antimicrobial and antibiofilm activities, J. Clust. Sci. 31 (2) (2020) 367–389.
[12] Y. Pan, C.J. Hurren, Q. Li, Effect of sonochemical scouring on the surface morphologies, mechanical properties, and dyeing abilities of wool fibres, Ultrason. Sonochem. 41 (2018) 227–233.
[13] T. Leong, M. Ashokkumar, S. Kentish, The fundamentals of power ultrasound - a review, Acoust. Aust. 39 (2) (2011) 54–63.
[14] L. Rayleigh, VIII. On the pressure developed in a liquid during the collapse of a spherical cavity, London, Edinburgh, Dublin Philos. Mag. J. Sci. 34 (200) (1917) 94–98.
[15] T.S.H. Leong, G.J.O. Martin, M. Ashokkumar, Ultrasonic encapsulation – a review, Ultrason. Sonochem. 35 (2017) 605–614.
[16] T.R. William, A.L. Loomis, The chemical effects of high frequencey sound waves I. A preliminary survey, J. Am. Chem. Soc. 49 (12) (1927) 3086–3100.
[17] S. Brohult, Splitting of the hæmocyanin molecule by ultra-sonic waves, Nature 140 (3549) (1937), 805-805.
[18] L.H. Thompson, L.K. Doraiswamy, Sonochemistry: science and engineering, Ind. Eng. Chem. Res. 38 (4) (1999) 1215–1249.
[19] T.J. Mason, J.P. Lorimer, D.M. Bates, Quantifying sonochemistry: casting some light on a 'black art', Ultrasonics 30 (1) (1992) 40–42.
[20] J.M. Pestman, J.B.F.N. Engberts, J.F. de, Sonochemistry: theory and applications, Recl. Trav. Chim. Pays-Bas 113 (12) (1994) 533–542.
[21] E. Salami, M. Salari, M. Ehteshami, S.N. Sheibani, Artificial neural network (ANN) modeling of cavitation mechanism by ultrasonic irradiation for cyanobacteria growth inhibition, Environ. Treat. Tech. 8 (2) (2020) 625–633.
[22] J.W. Kang, H.M. Hung, A. Lin, M. Hoffmann, Sonolytic destruction of methyl tert butyl ether by ultrasonic irradiation: the role of O3, H2O2, frequency, and power density, Environ. Sci. Technol. 33 (18) (1999) 3199–3205.
[23] R.Y. Zhang, Y. Huang, C.B. Sun, Z.L. Liang, X.S. Bentian, Z.J. Wang, Study on ultrasonic techniques for enhancing the separation process of membrane, Ultrason. Sonochem. 55 (2019) 341–347.
[24] A.A. Pykin, E.Y. Gornostaeva, N.P. Lukutsova, J.S. Pykina, Lightweight concrete based on gypseous binding materials, modified with microcrystalline cellulose, and cavitationly processed sawdust, Mater. Sci. Forum 945 (2019) 188–192.
[25] G.A. Grande, M. Giansetti, A. Pezzin, G. Rovero, S. Sicardi, Use of the ultrasonic cavitation in wool dyeing process: effect of the dye-bath temperature, Ultrason. Sonochem. 35 (2017) 276–284.
[26] A.J. Hu, S.T. Jiao, J. Zheng, L. Li, Y.S. Fan, L. Chen, Z.H. Zhang, Ultrasonic frequency effect on corn starch and its cavitation, LWT–Food Sci. Technol. 60 (2, Part 1) (2015) 941–947.
[27] J. Qiao, Y.R. Li, L.Q. Li, Ultrasound-assisted 3D printing of continuous fiber-reinforced thermoplastic (FRTP) composites, Addit. Manuf. 30 (2019), 100926.
[28] J.T. Han, J.I. Jang, H. Kim, J.Y. Hwang, H.K. Yoo, J.S. Woo, S. Cho, H.Y. Kim, H. J. Jeong, S.Y. Jeong, K.J. Baeg, K. Cho, G.W. Lee, Extremely efficient liquid exfoliation and dispersion of layered materials by unusual acoustic cavitation, Sci. Rep. 4 (1) (2014) 5133.
[29] M.L. Tsaih, L.Z. Tseng, R.H. Chen, Effects of removing small fragments with ultrafiltration treatment and ultrasonic conditions on the degradation kinetics of chitosan, Polym. Degrad. Stab. 86 (1) (2004) 25–32.
[30] M. Dükkanci, Ultrasonic degradation of oxalic acid in aqueous solutions, Ultrason. Sonochem. 13 (6) (2006) 517–522.
[31] L.F. Zhang, X.Q. Ye, X.J. Sophia, X.Z. Zhang, D.D. Liu, R.F. Meng, S.G. Chen, Effect of high-intensity ultrasound on the physicochemical properties and nanostructure of citrus pectin, J. Sci. Food Agric. 93 (8) (2013) 2028–2036.
[32] H.W. Hao, M.S. Wu, Y.F. Chen, J.W. Tang, Q.Y. Wu, Cavitation mechanism in cyanobacterial growth inhibition by ultrasonic irradiation, Colloids Surf. B 33 (3) (2004) 151–156.
[33] W.Y. Qiu, W.D. Cai, M. Wang, J.K. Yan, Effect of ultrasonic intensity on the conformational changes in citrus pectin under ultrasonic processing, Food Chem. 297 (2019), 125021.
[34] X.Q. Wang, Z.M. Yu, Y. Zhang, C.S. Qi, W.L. Chang, Evaluation of ultrasonic-assisted dyeing properties of fast-growing poplar wood treated by reactive dye based on grey system theory analysis, J. Wood Sci. 64 (6) (2018) 861–871.
[35] O. Rudak, B. Stefan, R. Pavel, C. Vadzim, Koleda Peter, densification of wood – chemical and structural changes due to ultrasonic and mechanical treatment, Bioresources 16 (4) (2021) 1–15.
[36] A.M. Basedow, K.H. Ebert, Ultrasonic Degradation of Polymers in Solution, Springer Berlin Heidelberg, Berlin, Heidelberg, 1977.
[37] J. Qian, Y.J. Li, J.J. Gao, Z.B. He, S.L. Yi, The effect of ultrasonic intensity on physicochemical properties of Chinese fir, Ultrason. Sonochem. 64 (2020), 104985.
[38] R. Koshani, S.M. Jafari, Ultrasound-assisted preparation of different nanocarriers loaded with food bioactive ingredients, Adv. Colloid Interface Sci. 270 (2019) 123–146.
[39] L. Feng, X.H. Li, W.C. Lu, Z. Liu, C. Xu, Y. Chen, H.L. Zheng, Preparation of a graft modified flocculant based on chitosan by ultrasonic initiation and its synergistic effect with kaolin for the improvement of acid blue 83 (AB 83) removal, Int. J. Biol. Macromol. 150 (2020) 617–630.
[40] A. Nouri, Y.M. Tavakkoli, A. Lajevardi, Z. Rezaei, M. Ghorbanpour, M. Tanzifi, Ultrasonic-assisted green synthesis of silver nanoparticles using Mentha aquatica leaf extract for enhanced antibacterial properties and catalytic activity, Colloid Interface Sci. Commun. 35 (2020), 100252.
[41] M. Rakshit, P.P. Srivastav, K. Bhunia, Kinetic modeling of ultrasonic-assisted extraction of punicalagin from pomegranate peel, J. Food Process Eng. 43 (11) (2020), e13533.
[42] A. Albermany, B. Kadem, F. Kadem, Study of some mechanical properties of PVA/ZnO composite by ultrasonic waves, J. Babylon Univ.Pure Appl. Sci. 21 (1) (2013) 244.
[43] H.A. Sabathini, L. Windiani, Dianursanti, M. Gozan, Mechanical physicial properties of chlorella-PVA based bioplastic with ultrasonic homogenizer, E3S Web Conf. 67 (2018), 03046.
[44] J. Amesimeku, L.H. Fan, W.Z. Jakpa, C.X. Wang, Dyeing properties of meta-aramid fabric dyed with basic dye using ultrasonic-microwave irradiation, J. Clean. Prod. 285 (2021), 124844.
[45] L. Johansson, T. Singh, T. Leong, R. Mawson, S. McArthur, M. Richard, J. Pablo, Cavitation and non-cavitation regime for large-scale ultrasonic standing wave particle separation systems – in situ gentle cavitation threshold determination and free radical related oxidation, Ultrason. Sonochem. 28 (2016) 346–356.
[46] T. Leong, L. Johansson, P. Juliano, S.L. McArthur, R. Manasseh, Ultrasonic separation of particulate fluids in small and large scale systems: a review, Ind. Eng. Chem. Res. 52 (47) (2013) 16555–16576.
[47] A. Albermany, A study of some mechanical properties of iraqi palm fiber-PVA composite by ultrasonic, Eur. J. Appl. Eng. Sci. Res. 61 (2) (2011) 1450.

[48] F. Lionetto, M. Alfonso, Polymer characterization by ultrasonic wave propagation, Adv. Polym. Technol. 27 (2) (2008) 63–73.
[49] S.M. Jafari, Y.H. He, B. Bhandar, Nano-emulsion production by sonication and microfluidization—a comparison, Int. J. Food Prop. 9 (3) (2006) 475–485.
[50] H.C. Wu, F.W. Shen, X. Hong, W.V. Chang, H. Winet, Monitoring the degradation process of biopolymers by ultrasonic longitudinal wave pulse-echo technique, Biomaterials 24 (22) (2003) 3871–3876.
[51] Y.G. Adewuyi, Sonochemistry: environmental science and engineering applications, Ind. Eng. Chem. Res. 40 (22) (2001) 4691–4715.
[52] H.Y. Yen, M.H. Yang, The ultrasonic degradation of polyacrylamide solution, Polym. Test. 22 (2) (2003) 129–131.
[53] D.L. Wang, X.B. Ma, L.F. Ya, T. Chantapakul, W.J. Wang, T. Ding, X.Q. Ye, D. H. Liu, Ultrasound assisted enzymatic hydrolysis of starch catalyzed by glucoamylase: investigation on starch properties and degradation kinetics, Carbohydr. Polym. 175 (2017) 47–54.
[54] C. Hernandez, L. Nieves, L.A. C. de, R. Advincula, A.A. Exner, Role of surface tension in gas nanobubble stability under ultrasound, ACS Appl. Mater. Interfaces 10 (12) (2018) 9949–9956.
[55] M.B. Ticha, W. Haddar, N. Meksi, A. Guesmi, M.F. Mhenni, Improving dyeability of modified cotton fabrics by the natural aqueous extract from red cabbage using ultrasonic energy, Carbohydr. Polym. 154 (2016) 287–295.
[56] B. Yang, Q.J. Wu, Y.X. Luo, Q. Yang, X.Y. We, J.Q. Kan, High-pressure ultrasonic-assisted extraction of polysaccharides from Hovenia dulcis: extraction, structure, antioxidant activity and hypoglycemic, Int. J. Biol. Macromol. 137 (2019) 676–687.
[57] J. Rooze, E.V. Rebrov, J.C. Schouten, J.T.F. Keurentjes, Dissolved gas and ultrasonic cavitation – a review, Ultrason. Sonochem. 20 (1) (2013) 1–11.
[58] Y. Iwai, S.C. Li, Cavitation erosion in waters having different surface tensions, Wear 254 (1) (2018) 1–9.
[59] L. Sheng, Y.B. Wang, J.H. Chen, J. Zou, Q. Wang, M.H. Ma, Influence of high-intensity ultrasound on foaming and structural properties of egg white, Food Res. Int. 108 (2018) 604–610.
[60] E. Camerotto, S. Brems, M. Hauptmann, A. Pacco, H. Struyf, P.W. Mertens, G. S. De, Influence of surface tension on cavitation noise spectra and particle removal efficiency in high frequency ultrasound fields, J. Appl. Phys. 112 (11) (2012), 114322.
[61] Y.P. Zhang, N. Zhang, Q. Wang, P. Wang, Y.Y. Yu, A facile and eco-friendly approach for preparation of microkeratin and nanokeratin by ultrasound-assisted enzymatic hydrolysis, Ultrason. Sonochem. 68 (2020), 105201.
[62] D. Vallejo-Domínguez, E. Rubio-Rosas, E. Aguila-Almanza, H. Hernández-Cocoletzi, M.E. Ramos-Cassellis, M.L. Luna-Guevara, K. Rambabu, S. Manickam, H.M.H. Siti, S.P. Loke, Ultrasound in the deproteinization process for chitin and chitosan production, Ultrason. Sonochem. 72 (2021), 105417.
[63] P. Krishnaiah, C.T. Ratnam, S. Manickam, Enhancements in crystallinity, thermal stability, tensile modulus and strength of sisal fibres and their PP composites induced by the synergistic effects of alkali and high intensity ultrasound (HIU) treatments, Ultrason. Sonochem. 34 (2017) 729–742.
[64] H.Y. Chen, J. Qin, Y. Hu, Efficient degradation of high-molecular-weight hyaluronic acid by a combination of ultrasound, hydrogen peroxide, and copper ion, Molecules 24 (3) (2019) 617.
[65] Y. Zhang, H. Ding, Y.F. Wu, C.X. Zhang, H.T. Wang, B.L. Bai, Ultrasound-induced controllable morphology and growth dimension in a dihydrazide-based self-assembly system, Soft Matter 10 (2014) 8838–8845.
[66] N.F.M. Noor, S.F.M. Yusoff, Ultrasonic-enhanced synthesis of rubber-based hydrogel for waste water treatment: kinetic, isotherm and reusability studies, Polym. Test. 81 (2020), 106200.
[67] T. Vu, Y. Xue, T. Vuong, M. Erbe, C. Bennet, B. Palazzo, L. Popielski, N. Rodriguez, X. Hu, Comparative study of ultrasonication-induced and naturally self-assembled silk fibroin-wool keratin hydrogel biomaterials, Int. J. Mol. Sci. 17 (9) (2016) 1497.
[68] M.M. Iftime, A. Marian, Ultrasonication-a potential method toward chitosan hydrogels, Mater. Plast. 57 (2020) 67–77.
[69] B. Rokita, J.M. Rosiak, P. Ulanski, Ultrasound-induced cross-linking and formation of macroscopic covalent hydrogels in aqueous polymer and monomer solutions, Macromolecules 42 (9) (2009) 3269–3274.
[70] Y.J. Wang, X. Zhang, D. Qiu, Y. Li, L.H. Yao, J.K. Duan, Ultrasonic assisted microwave synthesis of poly (Chitosan-co-gelatin)/polyvinyl pyrrolidone IPN hydrogel, Ultrason. Sonochem. 40 (2018) 714–719.
[71] Y. Yang, G. Greco, D. Maniglio, B. Mazzolai, C. Migliaresi, N. Pugno, A. Motta, Spider (Linothele megatheloides) and silkworm (Bombyx mori) silks: comparative physical and biological evaluation, Mater. Sci. Eng. C 107 (2020), 110197.
[72] J. Li, Z. Hu, L. Tan, Z.X. Jiang, L. Liu, Y.D. Huang, Preparation and properties of PIPD nanofibers made by a swelling and ultrasonic stripping process, RSC Adv. 6 (24) (2016) 78073–78079.
[73] Q. Wang, X.X. Yan, Y.J. Chang, L.L. Ren, J. Zhou, Fabrication and characterization of chitin nanofibers through esterification and ultrasound treatment, Carbohydr. Polym. 180 (2018) 81–87.
[74] S.S. Singh, L.T. Lim, A. Manickavasagan, Ultrasound-assisted alkali-urea pre-treatment of miscanthus × giganteus for enhanced extraction of cellulose fiber, Carbohydr. Polym. 247 (2020), 116758.
[75] Y. Lu, Q.F. Sun, X.L. She, Y.Z. Xia, Y.X. Liu, J. Li, D.J. Yang, Fabrication and characterisation of α-chitin nanofibers and highly transparent chitin films by pulsed ultrasonication, Carbohydr. Polym. 98 (2) (2013) 1497–1504.
[76] I.A. Gilca, V.I. Popa, C. Crestini, Obtaining lignin nanoparticles by sonication, Ultrason. Sonochem. 23 (2015) 369–375.
[77] S. Ventura-Cruz, A. Tecante, Nanocellulose and microcrystalline cellulose from agricultural waste: review on isolation and application as reinforcement in polymeric matrices, Food Hydrocoll. 118 (2021), 106771.
[78] Q.Q. Deng, F. Wang, C.R. Gough, X. Hu, Tunable microphase-regulated silk fibroin/poly (lactic acid) biocomposite materials generated from ionic liquids, Int. J. Biol. Macromol. 197 (2022) 55–67.
[79] Q.C. Liu, F. Wang, Z.G. Gu, Q.Y. Ma, X. Hu, Exploring the structural transformation mechanism of Chinese and Thailand silk fibroin fibers and formic-acid fabricated silk films, Int. J. Mol. Sci. 19 (11) (2018) 3309.
[80] F. Wang, A.S.S. Jyothirmayee, H. Wu, J. Forys, V. Venkatarama, K. Ramanujachary, X. Hu, Tunable green graphene-silk biomaterials: mechanism of protein-based nanocomposites, Mater. Sci. Eng. C. 79 (2017) 728–739.
[81] S. Samal, D. Kaplan, E. Chiellini, Ultrasound sonication effects on silk fibroin protein, Macromol. Mater. Eng. 298 (2013) 1201–1208.
[82] G.P. Guo, Q.Y. Ma, B. Zhao, D. Zhang, Ultrasound-assisted permeability improvement and acoustic characterization for solid-state fabricated PLA foams, Ultrason. Sonochem. 20 (1) (2013) 137–143.
[83] F. Chen, L. Xie, Enhanced fouling-resistance performance of polypropylene hollow fiber membrane fabricated by ultrasonic-assisted graft polymerization of acrylic acid, Appl. Surf. Sci. 502 (2020), 144098.
[84] A.I. Susanin, E.S. Sashina, V.V. Zakharov, M. Zaborski, D.A. Kashirskii, Conformational transitions of silk fibroin in solutions under the action of ultrasound, Russ. J. Appl. Chem. 91 (7) (2018) 1193–1197.
[85] G. Carissimi, A.A. Lozano-Pérez, M.G. Montalbán, S.D. Aznar-Cervantes, L. Cenis José, G. Víllora, Revealing the influence of the degumming process in the properties of silk fibroin nanoparticles, Polymers 11 (12) (2019) 2045.
[86] Z.Y. Li, J.Y. Wang, B.D. Zheng, Z.B. Guo, Impact of combined ultrasound-microwave treatment on structural and functional properties of golden threadfin bream (Nemipterus virgatus) myofibrillar proteins and hydrolysates, Ultrason. Sonochem. 65 (2020), 105063.
[87] P. Krishnaiah, R.C. Thevy, S. Manickam, Morphology water absorption and biodegradable properties of polylactide biocomposites reinforced with sisal fibers, Mater. Today: Proc. 5 (10, Part 3) (2018) 22506–22516.
[88] P.C.S. Faria Tischer, M.R. Sierakowski, H. Westfahl, C.A. Tischer, Nanostructural reorganization of bacterial cellulose by ultrasonic treatment, Biomacromolecules 11 (5) (2010) 1217–1224.
[89] I.H.P. Andrade, C.G. Otoni, T.S. Amorim, G.P. Camilloto, R.S. Cruz, Ultrasound-assisted extraction of starch nanoparticles from breadfruit (Artocarpus altilis (Parkinson) Fosberg), Colloids Surf. A Physicochem. Eng. Asp. 586 (2020), 124277.
[90] J. Zheng, Q. Li, A.J. Hu, L. Yang, J. Lu, X.Q. Zhang, Q.Q. Lin, Dual-frequency ultrasound effect on structure and properties of sweet potato starch, Starch - Stärke 65 (7–8) (2013) 621–627.
[91] A.F.K. Minakawa, P.C.S. Faria-Tischer, S. Mali, Simple ultrasound method to obtain starch micro- and nanoparticles from cassava, corn and yam starches, Food Chem. 283 (2019) 11–18.
[92] A.P. Teodoro, S. Mali, N. Romero, G.M. de Carvalho, Cassava starch films containing acetylated starch nanoparticles as reinforcement: physical and mechanical characterization, Carbohydr. Polym. 126 (2015) 9–16.
[93] N.A.M. Ishak, I. Khalil, F.Z. Abdullah, J.N. Muhd, A correlation on ultrasonication with nanocrystalline cellulose characteristics, Carbohydr. Polym. 246 (2020), 116553.
[94] R.J. Qu, M. Tang, Y. Wang, D. Li, L.J. Wang, TEMPO-oxidized cellulose fibers from wheat straw: effect of ultrasonic pretreatment and concentration on structure and rheological properties of suspensions, Carbohydr. Polym. 255 (2021), 117386.
[95] X.G. Li, L.Y. Wu, M.R. Huang, H.L. Shao, H.X. Chao, Conformational transition and liquid crystalline state of regenerated silk fibroin in water, Biopolymers 89 (6) (2010) 497–505.
[96] D.X. Xu, L.P. Feng, Y.P. Cap, J.S. Xiao, Impact of ultrasound on the physical properties and interaction of chitosan-sodium alginate, J. Dispers. Sci. Technol. 37 (3) (2016) 423–430.
[97] D.L. Wang, F.R. Hou, X.B. Ma, W.J. Chen, L.F. Yan, T. Ding, X.Q. Ye, D.H. Liu, Study on the mechanism of ultrasound-accelerated enzymatic hydrolysis of starch: analysis of ultrasound effect on different objects, Int. J. Biol. Macromol. 148 (2020) 493–500.
[98] M. Sujka, J. Jamroz, Ultrasound-treated starch: SEM and TEM imaging, and functional behaviour, Food Hydrocoll. 31 (2) (2013) 413–419.
[99] M. Asrofi, H. Abral, A. Kasim, A. Pratoto, M. Mahardika, F. Hafizulhaq, Mechanical properties of a water hyacinth nanofiber cellulose reinforced thermoplastic starch bionanocomposite: effect of ultrasonic vibration during processing, Fibers 6 (2) (2018) 40.
[100] A. Estrada-Monje, R. Zitzumbo-Guzmán, J.A. Bañuelos-Díaz, E.A. Zaragoza-Contreras, Ultrasonic dispersion and activation of TiO2 nanoparticles and its effect on bacterial inhibition in EVA films, Mater. Chem. Phys. 235 (2019), 121760.
[101] W.T. Lan, S.Y. Li, S.T. Shama, Y.Q. Zhao, D.E. Sameen, L. He, Y.W. Liu, Investigation of ultrasonic treatment on physicochemical, structural and morphological properties of sodium Alginate/AgNPs/Apple polyphenol films and its preservation effect on strawberry, Polymers 12 (9) (2020), 2096.
[102] X. Lin, S.W. Sun, B.L. Wang, B.D. Zheng, Z.B. Guo, Structural and physicochemical properties of lotus seed starch nanoparticles prepared using ultrasonic-assisted enzymatic hydrolysis, Ultrason. Sonochem. 68 (2020), 105199.

[103] A.R. Jambrak, Z. Herceg, D. Šubarić, J. Babić, M. Brnčić, S.R. Brnčić, T. Bosiljkov, D. Čvek, B. Tripalo, J. Gelo, Ultrasound effect on physical properties of corn starch, Carbohydr. Polym. 79 (1) (2010) 91–100.
[104] B. Gielen, J. Jordens, L. Thomassen, L. Braeken, G.T. Van, Agglomeration control during ultrasonic crystallization of an active pharmaceutical ingredient, Crystals 7 (2017) 40.
[105] J.G. Martinez-Colunga, S. Sanchez-Valdes, L.F. Ramos-deValle, E. Ramirez-Vargas, C. AvilaOrta, J.A. Rodriguez-Gonzalez, C.J. Espinoza-González, R. Benavides-Cantú, T. LozanoRamírez, Effect of ultrasonic irradiation on low-density polyethylene molecular structure, Polym. Bull. 77 (10) (2020) 5303–5321.
[106] V. Desai, M.A. Shenoy, P.R. Gogate, Ultrasonic degradation of low-density polyethylene, Chem. Eng. Process. Process Intensif. 47 (9) (2008) 1451–1455.
[107] N. Khan, J.Y. Pu, C.S. Pu, H.X. Xu, X.Y. Gu, L. Zhang, F.F. Huang, N.M. Ali, U. Rooh, Experimental and mechanism study: partially hydrolyzed polyacrylamide gel degradation and deplugging via ultrasonic waves and chemical agents, Ultrason. Sonochem. 56 (2019) 350–360.
[108] E.Y. Wardhono, H. Wahyudi, S. Agustina, F. Oudet, M.P. Pinem, D. Clausse, K. Saleh, E. Guénin, Ultrasonic irradiation coupled with microwave treatment for eco-friendly process of isolating bacterial cellulose nanocrystals, Nanomaterials 8 (10) (2018) 859.
[109] J. Hafsa, M.A. Chaouch, B. Charfeddine, C. Rihouey, H. Majdoub, Effect of ultrasonic degradation of hyaluronic acid extracted from rooster comb on antioxidant and antiglycation activities, Pharm. Biol. 55 (1) (2017) 156.
[110] S. Boufi, H.S. Bel, A. Magnin, F. Pignon, M. Impéror-Clerc, G. Mortha, Ultrasonic assisted production of starch nanoparticles: structural characterization and mechanism of disintegration, Ultrason. Sonochem. 41 (2018) 327–336.
[111] I. Yasuo, T. Tuziuti, K. Yasui, A. Towata, T. Kozuka, Control of viscosity in starch and polysaccharide solutions with ultrasound after gelatinization, Innov. Food Sci. Emerg. Technol. 9 (2) (2008) 140–146.
[112] N. Raoufi, R. Kadkhodaee, Y.P. Fang, G.O. Phillips, Ultrasonic degradation of Persian gum and gum tragacanth: effect on chain conformation and molecular properties, Ultrason. Sonochem. 52 (2019) 311–317.
[113] M. Sujka, Ultrasonic modification of starch – impact on granules porosity, Ultrason. Sonochem. 37 (2017) 424–429.
[114] Y.C. Cheung, J.Y. Yin, J.Y. Wu, Effect of polysaccharide chain conformation on ultrasonic degradation of curdlan in alkaline solution, Carbohydr. Polym. 195 (2018) 298–302.
[115] H.Z. Zou, B.F. Lin, C.H. Xu, M.J. Lin, W. Zhan, Preparation and characterization of individual chitin nanofibers with high stability from chitin gels by low-intensity ultrasonication for antibacterial finishing, Cellulose 25 (2) (2018) 999–1010.
[116] H. Suryanto, S. Jenuardy, D. Kustono, R.A. Dharmabintara, J. Maulana, U. Yanuhar, The influence of ultrasonic wave treatment on the mechanical properties of nanoclay-reinforced starch biocomposite, IOP Conf. Ser.: Mater. Sci. Eng. 515 (2019), 012021.
[117] B.W. Cai, H.L. Gu, F. Wang, P. Kyle, Z.G. Gu, H. Xiao, Ultrasound regulated flexible protein materials: fabrication, structure and physical-biological properties, Ultrason. Sonochem. 79 (2021), 105800.
[118] R. Ghosh, A. Ramakrishna, G. Reena, A. Ravindra, A. Verma, Water absorption kinetics and mechanical properties of ultrasonic treated Banana fiber reinforced-vinyl Ester composites, procediaMater. Sci. 5 (2014) 311–315.
[119] W.J. Lan, L. Xue, W.T. Lan, A. Saeed, Y.W. Liu, W. Qin, Electrospun polyvinyl Alcohol/d-limonene fibers prepared by ultrasonic processing for antibacterial active packaging material, Molecules 24 (2019) 767.
[120] Y.W. Liu, S.Y. Wang, W.J. Lan, W. Qin, Development of ultrasound treated polyvinyl alcohol/tea polyphenol composite films and their physicochemical properties, Ultrason. Sonochem. 51 (2019) 386–394.
[121] R. Serôdio, S.L. Schickert, A.R. Costa-Pinto, J.R. Dias, P.L. Granja, F. Yang, A. L. Oliveira, Ultrasound sonication prior to electrospinning tailors silk fibroin/PEO membranes for periodontal regeneration, Mater. Sci. Eng. C 98 (2019) 969–981.
[122] I. Kirsh, Y. Frolova, O. Bannikova, O. Beznaeva, I. Tveritnikova, D. Myalenko, V. Romanova, D. Zagrebina, Research of the influence of the ultrasonic treatment on the melts of the polymeric compositions for the creation of packaging materials with antimicrobial properties and biodegrability, Polymers 12 (2) (2020) 275.
[123] M. Pipathattakul, P. Surin, J. Wongon, Surface modification of sisal fibres by ultrasonic field, Key Eng. Mater. 728 (2017) 283–288.
[124] B.Q. Wang, P.H. Zhang, W.P. Song, L. Zhao, C.G. He, Modification of polyglycolic acid and poly lactic-co-glycolic acid fibers by ultrasonic treatment for enhancing hydrophilicity and cytocompatibility, J. Ind. Text. 45 (4) (2016) 516–530.
[125] M.S. Belluzo, L.F. Medina, A.M. Cortizo, M.S. Cortizo, Ultrasonic compatibilization of polyelectrolyte complex based on polysaccharides for biomedical applications, Ultrason. Sonochem. 30 (2016) 1–8.
[126] M. Asrofi, H. Abral, Y.K. Putra, S.M. Sapuan, H. Kim, Effect of duration of sonication during gelatinization on properties of tapioca starch water hyacinth fiber biocomposite, Int. J. Biol. Macromol. 108 (2018) 167–176.
[127] Y.K. Joung, B. Jang, J. Kang, D. Han, Precise ultrasonic coating and controlled release of sirolimus with biodegradable polymers for drug-eluting stent, Biomater. Biomed. Eng. 1 (2014) 13–25.
[128] P. Slepicka, K.N. Slepickova, S. Jakub, K. Zdenka, B. Lucie, S. Vaclav, Nano-structured and functionalized surfaces for cytocompatibility improvement and bactericidal action, Biotechnol. Adv. 33 (6) (2015) 1120–1129.
[129] S. Mohamadi Saani, J. Abdolalizadeh, H.S. Zeinali, Ultrasonic/sonochemical synthesis and evaluation of nanostructured oil in water emulsions for topical delivery of protein drugs, Ultrason. Sonochem. 55 (2019) 86–95.
[130] P. Khawas, S.C. Deka, Isolation and characterization of cellulose nanofibers from culinary banana peel using high-intensity ultrasonication combined with chemical treatment, Carbohydr. Polym. 137 (2016) 608–616.
[131] Y.S. Zhang, R.L. Jiang, A. Fang, Y.Y. Zhao, T.F. Wu, X.T. Cao, P.S. Liang, D.G. Xia, G.Z. Zhang, A highly transparent, elastic, injectable sericin hydrogel induced by ultrasound, Polym. Test. 77 (2019), 105890.
[132] P. Cass, K. Warren, P. Eliana, N.P. Holmes, T. Hughes, Preparation of hydrogels via ultrasonic polymerization, Ultrason. Sonochem. 17 (2) (2010) 326–332.
[133] M.T. Taghizadeh, A. Bahadori, Ultrasonic degradation of N-di and trihydroxy benzoyl chitosans and its effects on antioxidant activity, Ultrason. Sonochem. 21 (3) (2014) 1140–1149.
[134] K.M. Zia, S. Tabasum, M. Nasif, N. Sultan, N. Aslam, A. Noreen, M. Zuber, A review on synthesis, properties and applications of natural polymer based carrageenan blends and composites, Int. J. Biol. Macromol. 96 (2017) 282–301.
[135] Y. Shapovalova, D. Lytkin, L. Rasskazova, I. Zhuk, A. Gudima, A. Filimoshkin, N. Korotchenko, I. Kurzina, J. Kzhyshkowska, Preparation of biocompatible composites based on poly-L-Lactide/Hydroxyapatite and investigation of their anti-inflammatory activity, Key Eng. Mater. 683 (2016) 475–480.
[136] Y. Wang, T.G. Liu, B.R. Shah, Y. Li, B. Li, Ultrasonic treatment of α-chitin regenerated from a NaOH/urea solvent with tunable capacity for stabilization of oil in water emulsion, RSC Adv. 5 (107) (2015) 88316–88323.
[137] J.T. He, K.Q. Bian, G.Z. Piao, Self-assembly properties of carboxylated tunicate cellulose nanocrystals prepared by ammonium persulfate oxidation and subsequent ultrasonication, Carbohydr. Polym. 249 (2020), 116835.
[138] F.O. Ogutu, T.H. Mu, Ultrasonic degradation of sweet potato pectin and its antioxidant activity, Ultrason. Sonochem. 38 (2017) 726–734.
[139] Y.Y. Pu, Q.S. Zou, D.Z. Hou, Y.P. Zhang, S. Chen, Molecular weight kinetics and chain scission models for dextran polymers during ultrasonic degradation, Carbohydr. Polym. 156 (2017) 71–76.
[140] C.K. Lam, K. Lau, H. Cheung, H. Ling, Effect of ultrasound sonication in nanoclay clusters of nanoclay/epoxy composites, Mater. Lett. 59 (11) (2005) 1369–1372.
[141] Q.R. Xie, Y.C. Huang, Y.F. Ma, L. Qin, Study on the degradation of konjac glucomannan with ultrasonic, Food Sci. Technol. 9 (2006) 103–105.
[142] N.A. Patience, D. Schieppati, D.C. Boffito, Continuous and pulsed ultrasound pectin extraction from navel orange peels, Ultrason. Sonochem. 79 (2021), 105480.
[143] W. Chen, H.P. Yu, Y.X. Liu, P. Chen, M.X. Zhang, Y.F. Hai, Individualization of cellulose nanofibers from wood using high-intensity ultrasonication combined with chemical pretreatments, Carbohydr. Polym. 83 (4) (2011) 1804–1811.
[144] C.H. Li, S.Y. Liu, Y. Song, K. Nie, H.X. Ben, Y.M. Zhang, G.T. Han, W. Jiang, A facile and eco-friendly method to extract Apocynum venetum fibers using microwave-assisted ultrasonic degumming, Ind. Crop. Prod. 151 (2020), 112443.
[145] J.Q. Qiu, H. Zhang, Z.Y. Wang, Ultrasonic degradation of polysaccharides from Auricularia auricula and the antioxidant activity of their degradation products, LWT 113 (2019), 108266.
[146] R.B. Cui, F. Zhu, Effect of ultrasound on structural and physicochemical properties of sweetpotato and wheat flours, Ultrason. Sonochem. 66 (2020), 105118.
[147] H.W. Wang, K. Xu, Y. Ma, Y. Liang, H. Zhang, L. Chen, Impact of ultrasonication on the aggregation structure and physicochemical characteristics of sweet potato starch, Ultrason. Sonochem. 63 (2020), 104868.
[148] H. Abral, G.J. Putra, M. Asrofi, J.W. Park, H.J. Kim, Effect of vibration duration of high ultrasound applied to bio-composite while gelatinized on its properties, Ultrason. Sonochem. 40 (2018) 697–702.
[149] K.G. Akpomie, J. Conradie, Biogenic and chemically synthesized Solanum tuberosum peel–silver nanoparticle hybrid for the ultrasonic aided adsorption of bromophenol blue dye, Sci. Rep. 10 (1) (2020) 17094.
[150] M. Rasheed, M. Jawaid, B. Parveez, A. Zuriyati, A. Khan, Morphological, chemical and thermal analysis of cellulose nanocrystals extracted from bamboo fibre, Int. J. Biol. Macromol. 160 (2020) 183–191.
[151] E. Syafri, A. Kasim, H. Abral, A. Asben, Cellulose nanofibers isolation and characterization from ramie using a chemical-ultrasonic treatment, J. Nat. Fibers 16 (8) (2019) 1145–1155.
[152] S. Shabana, R. Prasansha, I. Kalinina, I. Potoroko, U. Bagale, S.H. Shirish, Ultrasound assisted acid hydrolyzed structure modification and loading of antioxidants on potato starch nanoparticles, Ultrason. Sonochem. 51 (2019) 444–450.
[153] T. Yuan, Z.X. Li, Y. Zhang, K. Shen, X. Zhang, R. Xie, F. Liu, W.M. Fan, Injectable ultrasonication-induced silk fibroin hydrogel for cartilage repair and regeneration, Tissue Eng. Part A 27 (2020) 17–18.
[154] V.S. Nguyen, D. Rouxel, R. Hadji, B. Vincent, Y. Fort, Effect of ultrasonication and dispersion stability on the cluster size of alumina nanoscale particles in aqueous solutions, Ultrason. Sonochem. 18 (1) (2011) 382–388.
[155] P.F. Liu, W. Gao, X.L. Zhang, B. Wang, F.X. Zou, B. Yu, L. Lu, Y.S. Fang, Z.Z. Wu, C. Yuan, B. Cui, Effects of ultrasonication on the properties of maize starch/stearic acid/sodium carboxymethyl cellulose composite film, Ultrason. Sonochem. 72 (2021), 105447.
[156] P.P. Borah, P. Das, L.S. Badwaik, Ultrasound treated potato peel and sweet lime pomace based biopolymer film development, Ultrason. Sonochem. 36 (2017) 11–19.

[157] P. Slepička, S. Jakub, L. Oleksiy, S.K. Nikola, K. Zdeňka, B. Lucie, Š. Václav, Polymer nanostructures for bioapplications induced by laser treatment, Biotechnol. Adv. 36 (3) (2018) 839–855.
[158] O. Neděla, P. Slepička, V. Švorčík, Surface modification of polymer substrates for biomedical applications, Materials 10 (10) (2017) 1115.
[159] L. Bacakova, J. Zarubova, M. Travnickova, J. Musilkova, J. Pajorova, P. Slepicka, N.S. Kasalkova, V. Svorcik, Z. Kolska, H. Motarjemi, M. Molitor, Stem cells: their source, potency and use in regenerative therapies with focus on adipose-derived stem cells – a review, Biotechnol. Adv. 36 (4) (2018) 1111–1126.